LASER INDUCED FLUORESCENCE STUDIES IN THE INDUCTIVELY COUPLED PLASMA

By

JOSEF B. SIMEONSSON

A DISSERTATION PRESENTED TO THE GRADUATE SCHOOL
OF THE UNIVERSITY OF FLORIDA IN PARTIAL FULFILLMENT
OF THE REQUIREMENTS FOR THE DEGREE OF
DOCTOR OF PHILOSOPHY

UNIVERSITY OF FLORIDA

1990

ACKNOWLEDGEMENTS

I want to express my love and gratitude to my mother, my father, my sister and Robin for their love and support, which have strengthened me and made this possible. I also want to add a much deserved thank you to Giuseppe, without whom I would not have made it through the last days. And I want to say thanks to Chris for answering all my small but time-consuming questions. I want to say thanks to Benny for the moral support and expert advice and to Jim of course, for giving me the opportunity to work with and learn from the best.

TABLE OF CONTENTS

ACKNOWLEDGEMENTS ii

ABSTRACT v

CHAPTER 1

INTRODUCTION 1

CHAPTER 2

HISTORY OF LASER EXCITED ATOMIC FLUORESCENCE 5

Laser Excited Atomic Fluorescence in Flames 5
LIF in Furnaces 14
ICP-LIF 15

CHAPTER 3

THEORY OF LASER EXCITED ATOMIC FLUORESCENCE . . . 18

Optical Saturation 18
Fluorescence Radiance 27
Spectral Selectivity 34
Saturation Broadening 36
Fluorescence Dip Spectroscopy 38

CHAPTER 4

EXPERIMENTAL 44

Instrumentation 44
Solutions 49

CHAPTER 5

ICP-LIF OF RARE EARTH ELEMENTS 51

Introduction 51
Results 53
Spectral Interferences 57

CHAPTER 6

SINGLE- AND DOUBLE-RESONANCE ICP-LIF 72

Introduction 72
Silver 75
Gold 79
Platinum 82
Palladium 90
Copper 94
Lead 97
Scandium 100
Analysis of Standard Reference Materials 104

CHAPTER 7

FLUORESCENCE DIP SPECTROSCOPY IN THE ICP 108

Introduction 108
Results 110
Time Dependent Fluorescence Dip Spectroscopy 147

CHAPTER 8

CONCLUSIONS 150

REFERENCE LIST 153

BIOGRAPHICAL SKETCH 159

Abstract of Dissertation Presented to the Graduate School
of the University of Florida in Partial Fulfillment of the
Requirements for the Degree of Doctor of Philosophy

LASER INDUCED FLUORESCENCE STUDIES IN THE INDUCTIVELY COUPLED PLASMA

By

Josef B. Simeonsson

December, 1990

Chairperson: James D. Winefordner
Major Department: Department of Chemistry

The application of laser induced fluorescence to the inductively coupled plasma (ICP-LIF) has been demonstrated as a method that is analytically sensitive and selective. Studies have been performed using both single resonance and double resonance laser excitation of ICP-LIF to evaluate the relative merits of the two techniques. Limits of detection are reported for Ag, Au, Ce, Cu, Dy, Er, Pb, Pd, Pt, Sc and Sm and range from sub-part-per-billion to tens of part-per-billion for both approaches. Consideration is also given to the concept of selectivity for the method of ICP-LIF, particularly to the relationship between the laser power and spectral selectivity for certain sample situations. A study of two rare earth elements, Dy and Gd, demonstrates the potential for increased spectral interferences caused by saturation broadening of the excitation profile and suggests that high power laser excitation can cause interferences.

In addition, ICP-LIF has been used to perform physical studies of excited state atomic transitions. The technique of fluorescence dip spectroscopy is presented as a demonstration of the unique diagnostic capabilities of ICP-LIF. The experimental results are used to determine selected parameters of excited state transitions and to evaluate the validity of a three level atom steady state model for Ag, Cu, Ir, Pb and Pd. Experimental results for copper atom are also used as an example of how time integrated fluorescence dip determinations can be used to evaluate Einstein coefficients and transition oscillator strengths of excited state transitions.

CHAPTER 1
INTRODUCTION

Trace analysis of metals is necessary for many geological, biological, chemical and environmental research applications. As understanding grows of chemical interactions at the microscopic levels, there is an increased need for highly sensitive and highly selective methods of analysis for metals at low concentration levels in a variety of sample types. Routine applications of trace metal analysis include plant and animal tissues, water samples, ore samples and semiconductor materials, with analyte concentrations ranging from the part-per-million (ppm) to the part-per-billion (ppb) level [1]. Standard methods of analysis include electrochemical methods, such as polarography and anodic stripping voltammetry, and spectrochemical methods, such as flame atomic absorption spectrometry, graphite furnace atomic absorption spectrometry and optical emission spectrometry in the inductively coupled plasma (ICP). Electrochemical methods are very sensitive but are hard to apply to complex and difficult samples. They often suffer serious interferences, are highly sensitive to changes in the sample matrix and are unsuitable for many types of samples. Spectrochemical methods, on the other hand, are viewed as more rugged and reliable and are capable of handling difficult samples with relative ease. Chemical interferences are less problematic, since the sample is atomized by high temperatures, and the selectivity of these optical methods is usually high.

For some applications, the standard methods of analysis are not suitable because of inadequate sensitivity or inadequate selectivity. An alternative spectrochemical method that was introduced in the early 1970s is laser induced fluorescence (LIF) or laser excited atomic fluorescence (LEAFS). LIF is a powerful spectroscopic method because of its "analytical duality" [2], which is the unique combination of high sensitivity and high selectivity. The application of LIF to flames, furnaces, plasmas and other atomizer cells has demonstrated repeatedly the analytical merits of the method. The application of LIF to electrothermal atomizers (ETA-LIF) in particular has resulted in absolute detection limits that are virtually unattainable by any other method. As the demand for high purity materials increases in the nuclear, semiconductor and biomedical industries, the need for techniques that can perform ultratrace analysis increases as well.

The application of LIF to ICPs has been proposed, but has not yet been fully explored for its full analytical potential. The ICP has long been regarded as an excellent atomizer cell for atomic and ionic emission spectrometry [3]. More recently, the ICP has been used very effectively as a source for ICP mass spectrometry [4,5]. The same virtues of ICP atomization that benefit ICP-ES and ICP-MS can also be utilized by LIF. The combination of the ICP with the "analytical duality" of LIF has great potential. Unlike LIF in other atomizers, ICP-LIF can be used to measure ionic as well as atomic fluorescence. ICP-LIF is also capable of performing analysis of refractory elements, for which most other methods are notoriously insensitive. ICP-LIF can be useful for determining elements for which spectral interferences are a common problem, primarily because of the high selectivity, which is characteristic of methods that use laser excitation. Classic examples of spectral interferences are analyses performed by ICP-ES of samples containing rare earth elements, which are important for nuclear and superconductor applications. The atomic and ionic emission spectra of many rare earth elements frequently overlap preventing accurate determinations by ICP-ES. ICP-LIF is an excellent method for such an application.

Another important aspect of ICP-LIF is the application to diagnostics, which receives little attention analytically, but is crucial for the complete understanding of many analytical spectroscopic methods. LIF, using either one or two lasers for optical excitation, is a valuable combustion diagnostic tool and provides important information about various flame species and processes including concentration and temperature profiles [6]. LIF has similar applications in plasmas and is well suited for ICP diagnostics. The simultaneous use of two lasers can provide spatial and spectral information about species in the ICP or about the plasma itself. The diagnostic capability of ICP-LIF can be exploited to increase the depth of knowledge spectroscopists have about plasma chemistry.

The purpose of these studies was to further develop and evaluate the spectroscopic method of ICP-LIF for analytical and diagnostic applications. A study of the rare earth elements using single resonance ICP-LIF was performed to determine the relative effectiveness of the technique in overcoming common spectral interferences. A comparison study of single resonance and double resonance fluorescence was performed to determine the relative analytical merits of the two methods. A study of fluorescence dip spectroscopy was done to demonstrate and evaluate ICP-LIF as a method for obtaining fundamental physical information.

CHAPTER 2
HISTORY OF LASER EXCITED ATOMIC FLUORESCENCE

Laser Excited Atomic Fluorescence in Flames

In 1968, R.M. Measures published a paper proposing future applications for what he called "selective excitation" spectroscopy [7]. Among these were diagnostic applications for plasmas such as electron temperatures, electron number densities, translational temperatures, particle velocities and magnetic field determinations based on Zeeman splitting. The study of atoms using "selective excitation" spectroscopy was also proposed and physical properties such as collision coupling rates and transition probabilities were suggested as parameters that potentially could be evaluated by such a technique. Schemes for performing these experiments were presented for potassium and barium atoms.

In 1971, both Denton and Malmstadt [8] as well as Fraser and Winefordner [9] independently reported the first application of lasers as excitation sources for analytical atomic spectrometry. To this point in time, atomic fluorescence spectrometry (AFS) was performed primarily with low power, continuous wave (CW) light sources, both line and continuum. These sources required modulation, either mechanical or electronic, to discriminate against background emissions, which are usually the primary noise source. Denton and Malmstadt, using a frequency doubled ruby laser to pump a dye laser, observed that the high peak power of the laser produced large scattering signals from water droplets in the flame. To remedy this, an ultrasonic nebulizer was used for sample introduction which improved the atomization efficiency of the flame and minimized laser scatter. Using this system, the authors were able to achieve fairly sensitive detection of barium atoms in a flame and demonstrate the use of a pulsed, tunable laser source for exciting atomic fluorescence.

Fraser and Winefordner used a nitrogen pumped dye laser in their initial studies. Their laser system had medium to low power outputs compared to present laser systems but was continuously tunable from 360 nm to 650 nm using a number of different dyes to cover the range. According to the authors, unlike conventional CW light sources, if a stable, high power, pulsed light source which has a narrow spectral bandwidth and a small duty cycle is used for excitation in AFS, the signal to noise ratio can be improved greatly over conventional source AFS. The short excitation pulse of such a source reduces the signal pulse duration and the duty cycle of the detector. The limiting noises in AFS are generally random noises such as dark current and flame background and analyte emissions and any reduction in the detector "on time" will reduce those noise contributions accordingly. The short pulses of a pulsed dye laser therefore are very nearly ideal for AFS. The laser used by Fraser and Winefordner was operated at 25 Hz and had a spectral bandwidth of approximately 0.1-1 nm FWHM. The light pulsewidths were typically 2 to 8 ns in duration. Based on their observations, the use of a pulsed dye laser allowed effective flame background discrimination. However, scattered laser radiation was a major noise contribution in these experiments. Another interesting conclusion resulted from these initial studies. The fluorescence spectral resolution of this method using dye laser excitation is determined directly by the laser (excitation) source and not by the detection spectrometer. The initial sensitivities were not superior to other methods but did compare favorably to those obtained by AFS using a conventional light source. The authors did note that the limited range of wavelengths available at the time prevented the excitation of strong resonance transitions for many elements below 360 nm, but could be reached by frequency doubling techniques in the future.

In 1972, Kuhl, Marowsky and Torge [10] reported the use of a flashlamp dye laser to analyze sodium in an absorption cell. This report is significant because it represents the first use of a dye laser for atomic absorption spectrometry. It also represents the first use of a dye laser whose output is narrowed to linewidths that are comparable to true elemental line source linewidths. The linewidth of this dye laser was reported as $5x10^{-4}$ nm. The absolute limit of detection of sodium by laser atomic absorption was determined to be about 2 ng. According to the authors, the main advantage of using the dye laser source is that the dye laser is tunable which allows background interferences to be compensated for by small detunings of the laser. Interestingly enough, the authors found that using a pulsed dye laser source was no better for atomic absorption than a hollow cathode lamp because of the pulse to pulse variations. Instead, they came to the conclusion that a laser source could find much better application in AFS.

It was observed, almost from the beginning of AFS with pulsed laser excitation, that there was a nonlinear relationship between the laser power and the observed fluorescence signals, for sufficiently high laser powers. Piepmeier described a theory of saturated atomic fluorescence using pulsed laser excitation in 1972 [11]. Using conventional low power sources for AFS, fluorescence signals normally were observed to be linearly related to the source intensity. With pulsed laser excitation, the peak power achieved was high enough to saturate the absorption step which resulted in a nonlinear relationship between the source power and the fluorescence power observed. According to Piepmeier, using laser excitation, an optically saturated, or nearly saturated, dilute atom population in a flame will provide spontaneous emission (fluorescence) several orders of magnitude more intense than a population that was excited by a conventional low power source. In addition, the saturated population will show a much lower dependence on variation in the source intensity (or changes in the population of fluorescence quenching species) than an unsaturated population. The theory used to describe the laser saturated atom population is based on a rate equations approach, which assumes steady state conditions during the laser pulse.

The major conclusions of this theory are that for excitation spectral irradiances beyond the saturation spectral irradiance, the fluorescing atom population is only weakly dependent on factors such as the population of quenchers and variations in the laser power. Therefore, the fluorescence emission signal effectively reaches a maximum for high laser radiances and becomes increasingly less dependent on variations in the source for even higher irradiances. However, even after the fluorescence has reached a maximum, the laser scatter will continue to increase linearly with the source irradiance and the fluorescence to scatter ratio will decrease with increasing laser powers. The theory suggested that there is an optimum laser source irradiance which provides saturated fluorescence emission signals with a minimum of laser induced scatter.

Also in 1972, Fraser and Winefordner [12] again reported results for laser excited atomic fluorescence spectrometry (LEAFS) experiments in a flame atomizer. In this report the authors discussed the major types of AFS that can be observed using laser excitation and they also detailed the experimental system used to perform their experiments and gave special attention to the modification in the photomultiplier tube necessary to perform gated detection using a pulsed laser source. The results obtained in these experiments included detection limits for thirteen different elements as well as some general conclusions based on their experimental observations. For resonance fluorescence measurements, the signal to noise ratio at high concentrations was primarily dependent on the shot noise of the detector, the pulse variations in the source output and laser scatter from the flame. At low concentrations, the signal to noise ratio was limited primarily by laser scatter, as was suggested by Piepmeier, and reduction of the scatter apparently would lower the detection limits. In addition, this paper reported the first analytical measurement of a two photon excited AFS signal, observed for cadmium and zinc solutions in a flame. Two photon excited AFS is only possible using laser excitation and recently the technique has found significant application in flame diagnostics [13-21].

In 1973, Omenetto et al. [22] reported the results of analytical studies of nine transition elements using LEAFS in a nitrous oxide-acetylene flame. This study was the first report of AFS measurements being performed for several of the elements which demonstrated the usefulness of a high intensity, tunable light source when a line source is not suitable or even available. The observation of strong nonresonance fluorescence emission for these elements was important because it allowed fluorescence measurements while avoiding scatter noises at the excitation wavelength.

Also in 1973, Omenetto et al. [23] published a paper similar to the theoretical paper published by Piepmeier [11] on saturated atomic fluorescence spectrometry. The major difference in the two theoretical treatments was the assumption of a monochromatic (line) source by Piepmeier and a quasi-continuum source by Omenetto et al. At the time, the assumption by Omenetto et al. was more realistic as the bandwidth of a typical dye laser was on the order of 0.1-1 nm and much larger than most atomic linewidths. The authors also presented experimental evidence that demonstrated the effects of optical saturation on the AFS signals observed which led to several conclusions about saturated atomic fluorescence spectrometry. As is expected, for low source irradiances, the fluorescence radiance is linearly related to the source intensity, but at high source irradiances, the fluorescence radiance becomes increasingly independent of the source intensity and reaches a maximum limit. The maximum fluorescence radiance observed is a property of the atom system and can be described by expressions derived from the theory presented in the paper. The authors also derived a general absolute expression which describes the relationship between the source flux for a continuum source and the fluorescence radiance produced, assuming steady state conditions for a two level atom system. The utility of this expression is that it holds true equally well at low and high source intensities. For saturation conditions produced by high source irradiances, the fluorescence radiance reaches a maximum which can be reduced to a simple expression in terms of the total atom population density, n_T. Determinations of the total atom population by saturated AFS measurements are beneficial because the measurements are independent of the quantum efficiency (i.e. independent of collision processes). Analytically this is important because the higher atomizing efficiency flames which use nitrous oxide are notorious for fluorescence quenching. This is not a concern for saturated fluorescence measurements as it is for fluorescence measurements which use low intensity light sources. As Piepmeier had previously concluded, the authors found that saturated fluorescence measurements are relatively independent of source fluctuations and therefore are less noisy. Unfortunately there is a significant trade off for working at source irradiances much greater than the saturation spectral irradiance. The laser scatter intensity was observed to increase linearly with the source intensity even when the fluorescence radiance has reached a maximum. Therefore, the authors concluded that the most effective way to compensate for laser scatter noise is to optimize the fluorescence signal to noise ratio rather than optimizing the signal alone since the scatter may be relatively more of a detriment when the fluorescence signal itself is at an optimum.

Boutilier et al. [24] published a paper in 1978 that detailed steady state atomic fluorescence radiance expressions for two and three level atoms excited by a continuum light source for saturating and non-saturating source irradiances. Two types of three level atoms were considered for the fluorescence radiance expressions that were derived. One case was for alkali-like atoms (i.e. sodium, potassium and cesium) when the uppermost two of the three energy levels are very close in energy and radiative transitions between those two levels are forbidden. The other case considered elements like indium and thallium where the three levels are all well separated in energy and radiative transitions are allowed from the two lower levels to the highest level but not between the two lower levels (i.e. the intermediate level is a metastable level). Following explicit derivations of all the possible radiative and nonradiative combinations for the two level and three level atoms, several conclusions were made about the fluorescence radiance expressions. For dilute atom vapors (low optical densities), the fluorescence radiance is linearly related to the total atom population for all source intensities. For two level atoms, the fluorescence radiance under saturation conditions is independent of collisional deactivation processes, but for any atom that cannot be accurately described as a two level system, the specific relationship of the fluorescence radiance to the total atom population requires some knowledge of the nonradiative relaxation rates (collisional deactivations).

In 1978, Weeks, Haraguchi and Winefordner [25] reported the results of a comprehensive study of 24 elements by LEAFS using flame atomization. Both resonance fluorescence and nonresonance fluorescence schemes were used for several of the elements for comparison purposes. While under ideal conditions, resonance fluorescence measurements will be limited by scattering from the laser source in the flame, for nonresonance fluorescence measurements, the limiting noise will be either the dark current, the amplifier noise, the flame background emission or molecular background fluorescence emission or a combination of some or all of these sources. If there is a strong nonresonance fluorescence scheme available for a given atom, then it is highly advantageous to do nonresonance measurements rather than resonance fluorescence measurements because of the lack of laser scatter noises. The results of the experiments performed demonstrated this for several elements and overall the detection limits reported in this study improved on the previous best (LEAFS) detection limits by up to 1 to 2 orders of magnitude. The authors felt that despite the apparently good results of this work, there was room for considerable improvement to be made for LEAFS as a method. Many of these improvements were centered on the use of a higher output power dye laser since the laser used in this study often operated too close to the saturation spectral energy density in the ultraviolet region which prevented the measurements from taking full advantage of saturated conditions. The use of an alternative atomizer was also suggested as a means of greatly reducing noise and improving the sensitivity of the method.

LIF in Furnaces

While LEAFS or laser induced fluorescence (LIF) in flames was enjoying moderate to good success, the search was ongoing for alternative atomizers to which LIF could be applied. As atomizers, flames suffer from several problems that prevent the application of LIF from achieving its potential in terms of sensitivity and selectivity. The susceptibility of flames to chemical and ionization interferences in addition to the characteristically low quantum efficiency of fluorescence in most flame gas mixtures redirected applications of LIF from flames to graphite furnaces, ICPs and other atomizer cells.

The application of LIF to furnace atomizers can be traced back to 1974 when Neumann and Kriese [26] reported the use of a flashlamp pumped dye laser that was frequency doubled to excite the 283.306 nm resonance absorption transition of lead. In this study, the relative performance of dye laser to hollow cathode lamp (HCL) and electrodeless discharge lamp (EDL) excitation was evaluated to determine the utility of LIF to nonflame atomizers. As the authors reported, the graphite furnace is a superior atomizer to flames for several reasons. The atom density in a furnace during the atomization cycle is exceptionally high and the furnace can be operated at high temperatures in an inert chemical environment. In addition, furnaces allow high sensitivity determinations for small samples. Even in this early report, an absolute detection limit of 0.2 pg was achieved using LIF in a graphite atomizer. Laser excitation provided both superior detection limits and a superior linear dynamic range to any previous AFS determinations using conventional light sources.

Since then, LIF in furnaces has been used to determine many elements at extremely low levels and for several elements, the technique of electrothermal atomization (ETA) combined with LIF has produced the lowest limits of detection by any spectrochemical method of analysis to date [27-30]. The technique has been repeatedly demonstrated as highly sensitive and capable of handling small samples with complex matrices. The future of this technique is very promising and could lead to the achievement of the intrinsic limit of detection [31]. However, the technique is not without its problems. The number of elements that can be analyzed by ETA-LIF is currently limited and despite the use of an inert atmosphere, the technique is still prone to interferences and has poor sensitivity for refractory elements. Successful application of the technique to refractory elements and real samples in the future will most likely require vacuum atomization which entails a considerable increase in experimental complexity.

ICP-LIF

The ICP was first used as an atomizer for AFS by Montaser and Fassel [32] in 1976. The excitation was provided by EDLs and Osram lamps which the authors considered to be the best existing primary excitation sources and were the most intense sources available for transitions in the ultraviolet region. The authors reported good detection limits for cadmium, zinc and mercury and excellent selectivity with no adverse effects observed on analyte signals even for complex mixtures of up to 17 concomitant elements in the sample matrix. Since then, ICP-

AFS has been performed very successfully using HCL excitation. HCL excitation is effective for those elements that provide sufficient radiant intensity of a resonance transition in a hollow cathode discharge. There are many elements with HCLs that do not provide enough intensity and the sensitivity is lacking for ICP-AFS. HCL excitation also implies that the analyte must be in the neutral form. HCLs do not typically produce radiation corresponding to ionic transitions and are therefore not useful for excitation of ionic transitions.

Pollard et al. [33] reported in 1979 for the first time the application of a dye laser as an excitation source for ICP-AFS. Although the results were not very favorable using CW laser excitation, excellent linearity of the fluorescence was observed and it was suggested that pulsed laser excitation could greatly improve the sensitivity of the method. The technique was also suggested as a useful way to perform plasma diagnostics in the ICP.

Epstein et al. [34] followed in 1980 with the study of both a flashlamp dye laser and a nitrogen pumped dye laser as excitation sources for ICP-AFS. The results of this study also did not compare favorably to established methods such as ICP-ES and flame AA. However, the authors emphasized that these were initial results and that simple modifications could be made to enhance the sensitivity of this technique. The authors also agreed that the technique could be a very useful tool for plasma diagnostics.

In 1983, Kosinski et al. [35] reported the use of a modified ICP torch for ICP-LIF which resulted in detection limits for 12 elements that compared very well with those obtained by ICP-AFS with HCL excitation [36-38]. The sensitivity of ICP-LIF was still not as high as for ICP-ES; however, the selectivity was very good and could be valuable for trace analysis of real samples. The technique was observed to be relatively independent of any spectral interferences. Also the authors noted that ionic fluorescence measurements were extremely sensitive in the ICP both because of the high concentration of ions in the ICP for certain elements and because ions do not suffer ionization losses in fluorescence as atoms often do in the ICP or in flames. Measurement of ionic fluorescence typically means that the ICP can be operated at higher powers providing better atomization efficiencies and better plasma stability. Ionic fluorescence is not a possibility for conventional line source excitation and this represents a distinct advantage that ICP-LIF has over conventional source ICP-AFS.

ICP-LIF has yet to be fully developed as an analytical tool or as a tool for plasma diagnostics. Past research has directed study towards the development of ICP-LIF to better exploit the unique atomizer qualities of the ICP with the high sensitivity and selectivity of LIF. The studies in this dissertation have concentrated on furthering the development of ICP-LIF, using single and dual dye laser excitation, both as an analytical method and as a tool for diagnostics in the ICP.

CHAPTER 3
THEORY OF LASER EXCITED ATOMIC FLUORESCENCE

Optical Saturation

The theory of atomic fluorescence spectrometry has been fully developed by other authors [39-41] and will not be treated in excessive detail at this time. As the studies performed for this work have used laser excitation exclusively, only those expressions directly relevant to laser excited atomic fluorescence (LEAFS) (or laser induced fluorescence (LIF)) will be discussed. To be specific, the principles of optical saturation, the quantum efficiency of fluorescence, fluorescence radiance, saturation broadening and fluorescence dip spectroscopy will each be presented in terms of a rate equations approach to atom level populations.

In most cases, the rate equations approach [42,43] is a valid way to address the theory of LEAFS (LIF). Using a simple two level atom as a model (Figure 1), the population densities of each of the two levels are described in terms of the rates of radiative and nonradiative processes that contribute to or detract from the level population. The rate equations approach assumes that the atom population being considered is a dilute species in a gas that typically is at atmospheric pressure. In the absence of any externally applied fields, the atoms are distributed between the two

Figure 1. Diagram of a two level atom.

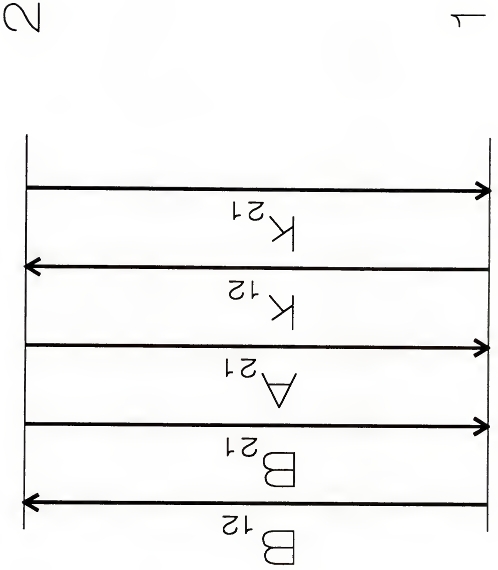
B_{12}
B_{21}
A_{21}
K_{12}
K_{21}
1
2

energy levels according to the Boltzmann distribution [44] which is dictated by the energy separation of the two levels, hν ,and the temperature of the system , T (°K):

$$\frac{n_2}{n_1} = \frac{g_2}{g_1} \exp\left(-\frac{h\nu}{kT}\right) \tag{1}$$

where h is Planck's constant (Js), ν is the frequency of the transition between levels 1 and 2 (Hz), k is Boltzmann's constant (JK^{-1}), g_i (i = 1 or 2) is the statistical weight of the level i and n_i (i = 1 or 2) is the population density of level i. The rate of decay of atoms from level 2 in the absence of collisions can be written as

$$\frac{dn_2}{dt} = -n_2 A_{21} \tag{2}$$

where A_{21} is the Einstein coefficient for spontaneous emission (s^{-1}).

When a laser is used to stimulate the atom population, the level population densities respond according to the radiative power of the laser excitation. The rates of excitation, R_{12} ($s^{-1}cm^3$), and relaxation, R_{21} ($s^{-1}cm^3$), between the two levels can be written as follows:

$$R_{12} = (B_{12}\rho(\nu_{12}) + k_{12})n_1 \tag{3}$$

$$R_{21} = (B_{21}\rho(\nu_{12}) + k_{21} + A_{21})n_2 \tag{4}$$

where B_{12} (Jcm^3Hzs^{-1}), B_{21} (Jcm^3Hzs^{-1}) and A_{21} (s^{-1}) are the Einstein coefficients for induced absorption, induced emission and spontaneous emission respectively, $\rho(\nu)$ is the spectral energy density of the laser and k_{12} and k_{21} (s^{-1}) are the rates of collisional excitation and collisional deexcitation respectively.

It will be useful to recall throughout the following equations the mathematical relationships of the Einstein coefficients to each other:

$$g_1B_{12} = g_2B_{21} \tag{5}$$

$$A_{21} = \frac{8\pi h\nu_{12}^3}{c^3}B_{21} = DB_{21} \tag{6}$$

$$\begin{gathered} \textit{and for } g_1 = g_2 \\ B_{12} = B_{21} = B \end{gathered} \tag{7}$$

$$\textit{and } k_{21} = k_{12}\exp(h\nu/kT) \tag{8}$$

In most cases k_{12} will be considered negligible.

The changes in the population density of level 2 as a function of time can be written as the sum of the forward and reverse rate equations:

$$\frac{dn_2}{dt} - n_1 B_{12}\rho(\nu) - n_2(B_{21}\rho(\nu) + k_{21} + A_{21}) \tag{9}$$

The solution to this differential equation gives the population density of level 2, n_2, in terms of the total atom population density, n_T (for $g_1 = g_2$) :

$$n_2(t) - n_T B\rho(\nu) t_r (1 - \exp(-\frac{t}{t_r})) \tag{10}$$

$$\textit{where } t_r - (2B\rho(\nu) + k_{21} + A_{21})^{-1} \tag{11}$$

and t_r (s) is known as the response time (or the pumping time) of the atom population to the induced absorption/emission. It is clear from this equation that for $B_{12}\rho(\nu)$ sufficiently large (and $g_1 = g_2$), equation 7 reduces to

$$n_2(\max) - \frac{n_T}{2} \tag{12}$$

If $g_1 \neq g_2$, then the equation takes the form

$$n_2(\max) - n_T \left(\frac{g_2}{g_1 + g_2} \right) \tag{13}$$

The saturation spectral energy density, $\rho_\nu^s(\nu)$ (J/cm^{3}Hz^{-1}), is defined (for $g_1 = g_2$) as

$$\rho_\nu^s(\nu) - \frac{A_{21} + k_{21}}{2B} \tag{14}$$

By substituting this value into equation 7, it is found that $\rho_\nu^s(\nu)$ is the spectral energy density that produces a population density in level 2 equal to one half the maximum population density achieved for saturated steady state conditions. By further inspection of these equations, the role of collisions in LEAFS or LIF becomes evident. From equation 7, it can be seen that the response time of the system is inversely proportional to the rate of collisional deactivation of level 2, k_{21}. It is intuitive that the spectral energy density required to achieve the maximum steady state population will increase as the rate of collisional deactivation increases. As the total rate of loss or depopulation of level 2 increases (radiative and nonradiative decay), the energy that must be supplied to compensate for those losses must also increase.

At this point, it is useful to define another parameter which directly represents the relative rate of radiative deactivation to collisional deactivation for a given level population, which is known as the quantum efficiency. The Stern-Volmer formula for the quantum efficiency of fluorescence, Y_{21}, is defined as

$$Y_{21} = \frac{A_{21}}{\textit{total probability of deactivation level } 2\ (s)^{-1}} \qquad (15)$$

$$Y_{21} = \frac{A_{21}}{A_{21} + k_{21}} \qquad (16)$$

In this formula, it is assumed that the atoms are excited from level 1 to level 2 by photon absorption and that deactivation may occur by collisions from level 2 to any level above or below level 2 or by radiative relaxation from level 2 to any level below level 2. The quantum efficiency is a direct indication of the probability that photon absorption by the atom which excites the atom from level 1 to level 2 will result in a radiative relaxation from level 2 to level 1 (fluorescence emission). Again, it is intuitive that the higher the rate of collisional deactivation or the greater the number of possible routes of collisional deactivation, the lower the probability of radiative relaxation (i.e., the lower the probability of fluorescence). The quantum efficiency can also be defined in terms of the lifetime of the level in the presence and in the absence of collisions. τ_{sp} is the lifetime of the level in the absence of collisions and is simply the inverse of A_{21}

$$\tau_{sp} = \frac{1}{A_{21}} \tag{17}$$

When collisions are present, it is easy to see that the sum of the radiative and nonradiative rates of relaxation will serve to increase the total rate of deactivation and the lifetime of the level will be reduced accordingly. The effective lifetime or observed lifetime of the level reflects this:

$$\tau_{eff} = \frac{1}{A_{21} + k_{21}} \tag{18}$$

$$\tau_{eff} < \tau_{sp} \tag{19}$$

The quantum efficiency of fluorescence, Y_{21}, can then be defined in terms of the lifetimes:

$$Y_{21} = \frac{\tau_{eff}}{\tau_{sp}} = \frac{A_{21}}{A_{21} + k_{21}} \tag{20}$$

The saturation spectral energy density is also related to the rate of collisional deactivation and therefore can be described in terms of the quantum efficiency or the effective lifetime. From equation 10,

$$\rho_{\nu}^{s}(\nu) = \frac{A_{21} + k_{21}}{2B} = \frac{A_{21}}{2By_{21}} = \frac{1}{2B\tau_{eff}} \tag{21}$$

In the absence of collisions,

$$\rho_{\nu}^{s}(\nu) = \frac{A_{21}}{2B} = \frac{1}{2B\tau_{sp}} \tag{22}$$

It is apparent from these equations that as k_{21} increases, Y_{21} will decrease and $\rho_{\nu}{}^{s}(\nu)$ will increase. For example, if $k_{21} = A_{21}$, then the quantum efficiency will be reduced in half and the saturation spectral energy density (the energy required to saturate the absorption transition) will increase by a factor of 2. Collisions therefore play an important role in determining several factors related to the saturation of an optical transition.

Fluorescence Radiance

For a two level atom system (Fig. 1), the fluorescence radiance, B_F, expression is given by the following equation:

$$B_F = n_2 A_{21} h\nu_{12}\left(\frac{L}{4\pi}\right) \tag{23}$$

To determine the ratio of n_2 to n_1 under steady state conditions, the rates of R_{12} and R_{21} (equations 3 and 4) can be set equal to one another:

$$R_{12} = R_{21} \tag{24}$$

$$n_1(B_{12}\rho(\nu) + k_{12}) = n_2(B_{21}\rho(\nu) + k_{21} + A_{21}) \tag{25}$$

$$\frac{n_2}{n_1} = \frac{(B_{12}\rho(\nu) + k_{12}}{(B_{21}\rho(\nu) + k_{21} + A_{21})} \tag{26}$$

$$\textit{Recalling that } D = \frac{8\pi h\nu_{12}^3}{c^3} \tag{27}$$

$$k_{21} = k_{12} \frac{g_1}{g_2} \exp\left(\frac{h\nu}{kT}\right) \tag{28}$$

$$\frac{n_2}{n_1} = \frac{g_2}{g_1}\left[\frac{[D(1-Y_{21})/Y_{21}]\exp(\frac{-h\nu}{kT}) + \rho(\nu)}{D/Y_{21} + \rho(\nu)}\right] \tag{29}$$

This expression is useful for describing the general behavior of a two level atom system to radiant excitation. When the spectral energy density of the source, $\rho(\nu)$, is equal to zero, the expression reduces to

$$\frac{n_2}{n_1} = \frac{g_2}{g_1} (1 - Y_{21}) \exp\left(\frac{-h\nu}{kT}\right) \tag{30}$$

which represents the deviation of the level populations from the Boltzmann distribution (radiative disequilibrium) and is characteristic of flames (or plasmas) that do not behave like Planck blackbody radiation sources (according to their temperatures). When $\rho(\nu)$ is equal to the energy density predicted by the Planck Radiation Law, the expression reduces to

$$\frac{n_2}{n_1} = \frac{g_2}{g_1} \exp\left(\frac{-h\nu}{kT}\right) \tag{31}$$

which is easily recognized as the Boltzmann equilibrium expression for the atom at temperature T. For very large values of $\rho(\nu)$, the expression approaches the limiting value where

$$\frac{n_2^{ss}}{n_1^{ss}} = \frac{g_2}{g_1} \tag{32}$$

This simple equation indicates what happens to the atom population for spectral energy densities that exceed the saturation value. At sufficiently large values of $\rho(\nu)$, the levels of the atom become populated according to the ratio of their respective statistical weights. For a two level atom under saturating radiant powers having $g_1 = g_2$, $n_2 = n_1$ and each level possesses one half of the total atom population. It is important to note that at saturation, the population of the levels is completely independent of both the source power and the quantum efficiency (the maximum populations are independent of collisional deactivation processes). The maximum fluorescence radiance under saturation conditions for a two level atom is

$$B_{F_{max}} = n_2^{ss} A_{21}\, h\nu_{12} \left(\frac{L}{4\pi}\right) \tag{33}$$

$$B_{F_{(max)}} = n_T \left(\frac{g_2}{g_1 + g_2}\right) A_{21}\, h\nu_{12} \left(\frac{L}{4\pi}\right) \tag{34}$$

For a three level atom (Figure 2) that experiences a two step excitation first from level 1 to level 2 and then from level 2 to level 3, the appropriate rate expressions are

$$R_{12} = B_{12}\rho(\nu_{12}) \tag{35}$$

Figure 2. Diagram of a three level atom.

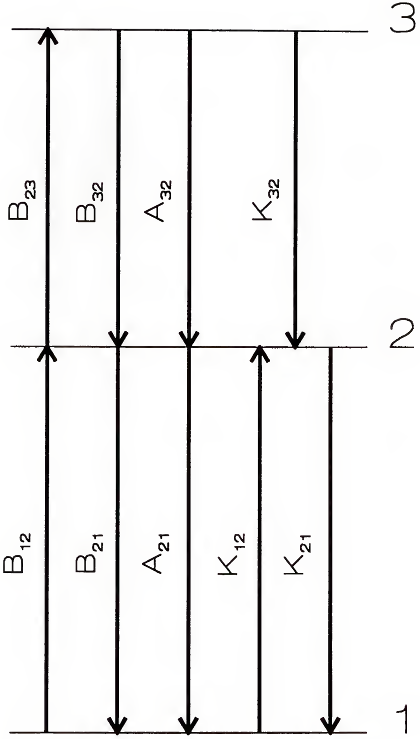
3
2
1
B_{23}
B_{32}
A_{32}
K_{32}
B_{12}
B_{21}
A_{21}
K_{12}
K_{21}

$$R_{23} = B_{23}\rho(\nu_{23}) \tag{36}$$

$$R_{13} = 0 \tag{37}$$

$$R_{21} = A_{21} + k_{21} + B_{21}\rho(\nu_{12}) \tag{38}$$

$$R_{32} = A_{32} + k_{32} + B_{32}\rho(\nu_{23}) \tag{39}$$

$$R_{31} = k_{31} \tag{40}$$

As in the case of the single step excitation just presented [equations 35-40] where an expression for n_2 was derived from the rate equations, it is possible to develop an equation that expresses the steady state population density of level 3, n_3, in terms of the rate equations for the total atom population density:

$$n_3 = \frac{B_{12}\rho(\nu_{12})B_{23}\rho(\nu_{23})n_T}{B_{12}\rho(\nu_{12})B_{23}\rho(\nu_{23})\left(\frac{g_1 + g_2 + g_3}{g_3}\right) + (A_{32} + k_{21} + k_{31})} \tag{41}$$

$$x\ \frac{1}{[(A_{21} + k_{21} + B_{21}\rho(\nu_{12})(1+\frac{g_1}{g_2})] + B_{32}\rho(\nu_{23})\cdot(A_{21} + k_{21} + k_{32}(\frac{g_3}{g_2}))} \tag{42}$$

For large values of both $B_{12}\rho(\nu_{12})$ and $B_{23}\rho(\nu_{23})$, which represents saturating spectral energy densities for lasers at both λ_{12} and λ_{23},the right hand side of this equation becomes relatively insignificant and the expression reduces to the following simple expression:

$$n_3^{sat} = n_T\left(\frac{g_3}{g_1 + g_2 + g_3}\right) \tag{43}$$

For saturating energy densities of the laser sources for each absorption, the population density of each level is once again dictated by the statistical weight of the level and each level shares a portion of the total atom population density according to the ratio of its statistical weight and the sum of the statistical weights of the three levels involved in the two transitions. The maximum fluorescence radiance expression from level 3 for a three level atom excited by a two step excitation or double resonance excitation scheme under saturation conditions can be written as

$$B_{F_{(max)}} = n_3^{sat}A_{32}\ h\nu_{23}\left(\frac{L}{4\pi}\right) \tag{44}$$

$$= n_T\left(\frac{g_3}{g_1 + g_2 + g_3}\right)A_{32}h\nu_{23}\left(\frac{L}{4\pi}\right) \tag{45}$$

The primary difference between this expression and the maximum fluorescence radiance expression for a singly excited two level atom is that the total atom population density is distributed among three levels rather than only two. In itself, this increased population distribution suggests that the maximum fluorescence radiance of the double resonance would be reduced relative to the maximum fluorescence radiance of the single resonance and would therefore reduce the sensitivity. However, by ratioing the two radiance expressions, as Omenetto et al. have done previously [45], and inspecting the equation,

$$\frac{B_{F_{(max)}}\ single}{B_{F_{(max)}}\ double} = \left(\frac{A_{21}\cdot\nu_{12}}{A_{32}\cdot\nu_{23}}\right)\left(\frac{g_2}{g_3}\right)\frac{(g_1 + g_2 + g_3)}{(g_1 + g_2)} \tag{46}$$

it is seen that double resonance fluorescence can produce radiances that are equal to those produced by single resonance excitation provided that the fluorescence emission transition is highly probable (large A_{32}), highly energetic (large $h\nu_{23}$) and proceeds from a level which is heavily populated (has a large statistical weight or large g_3). This implies that there will not necessarily be a loss in sensitivity for double resonance fluorescence relative to single resonance fluorescence provided these factors are true. This point will be addressed more specifically in Chapter 5 where its relevance is clear.

Spectral Selectivity

The selectivity advantage that LIF methods have over other optical methods of analysis is often referred to. The use of narrow linewidth dye lasers as excitation sources is primarily responsible for the high selectivity of LIF. When comparing the selectivities of various methods, it is useful to consider the total selectivity of a method, S_{total}, which can be thought of as the product of the selectivities of each step in the method:

$$S_{total} = S_1 \; x \; S_2 \; x \; S_3 \; ... \tag{47}$$

To illustrate the selectivity advantage of ICP-LIF over ICP-ES, for instance, relative selectivities can be calculated for each of the two methods for the determination of rare earth elements. The spectral selectivity of an optical method, S, can be defined as

$$S = \frac{R}{\Delta r} \tag{48}$$

where R is the range of all possible wavelengths and Δr is the spectral bandpass of the optically selective step or device. In ICP-ES, the selectivity of the method is determined in a single step by the detection process alone. Using typical values from Boumans et al. [46],

$$S = \frac{(535 \; nm \; - \; 180 \; nm)}{0.017 \; nm} \approx 20{,}000 \tag{49}$$

where R is the response range of the photomultiplier tube and Δr is the spectral bandpass of the spectrometer.

In ICP-LIF, spectral selectivity is obtained in both the excitation and detection steps.

$$\begin{aligned} S_{total} &= S_1 \; x \; S_2 \\ &= \frac{(750 \; nm \; - \; 250 \; nm)}{0.008 \; nm} \; x \; \frac{(800 \; nm \; - \; 180 \; nm)}{(1 \; mm \; x \; 2 \; nm/mm)} \\ &\approx 2 \; x \; 10^7 \end{aligned} \tag{50}$$

where S_1 and S_2 are the selectivities of the excitation and detection steps. R_1 is the spectral range of a typical dye laser and Δr_1 is the spectral bandwidth of the dye laser. R_2 is the spectral response range of the photomultiplier tube and Δr_2 is the spectral bandpass of the spectrometer for fluorescence detection. It is evident that while the detection selectivity of ICP-LIF is not as high as for ICP-ES, the selectivity of the excitation step is very high and the product of the two selectivities gives the method of ICP-LIF superior selectivity. While the selectivity of ICP-ES is adequate for most experimental situations, there are applications such as rare earth determinations that require higher selectivity. These equations show the great difference in spectral selectivities for ICP-LIF and ICP-ES. The importance of spectral selectivity will be referred to again in the study of the rare earth elements.

Saturation Broadening

When an atom is subjected to very high powers of laser radiation tuned to an atomic absorption line, the excitation profile (which is a convolution of the atomic linewidth and the laser bandwidth) is broadened as a function of the laser power [47-51]. There are various approaches that can be taken to modelling this laser/atom interaction and broadening phenomenon. The most applicable model is that of an atom profile which is described by a Gaussian function and a laser beam that also has a Gaussian profile [48]. The laser bandwidth is assumed to be either on the order of the atomic linewidth or larger. The laser spectral energy density profile is described by

$$\rho_\lambda(\lambda) = \rho_L \frac{2\sqrt{\ln 2}}{\sqrt{\pi \delta\lambda_L}} \exp\left(-\frac{2\sqrt{ln2}}{\sqrt{\delta\lambda_L}}(\lambda - \lambda_L)\right)^2 \qquad (51)$$

where ρ is the integrated energy density (J/cm^3) and $\delta\lambda_l$ is the laser bandwidth FWHM (nm). The atom profile is described by the shape function

$$g_\lambda^a(\lambda - \lambda_o) = \frac{2\sqrt{ln2}}{\sqrt{\pi\delta\lambda_a}} \exp\left(-\frac{2\sqrt{ln2}}{\delta\lambda_a}(\lambda - \lambda_o)\right)^2 \qquad (52)$$

where $\delta\lambda_a$ is the atom profile FWHM (nm). Since the atom and laser profiles are both Gaussian functions, the convolution of the two is also a Gaussian function and is given by the following equation:

$$\Sigma\rho_\lambda(\lambda)\cdot g_\lambda^a(\lambda - \lambda_o)d\lambda = \qquad (53)$$

$$\rho_L \frac{2\sqrt{ln2}}{\sqrt{\pi\delta\lambda'}} \exp\left(-\frac{2\sqrt{ln2}}{\delta\lambda'}(\lambda_L - \lambda_o)\right)^2 \qquad (54)$$

where $\delta\lambda'$ is the effective bandwidth (nm) which is the convolution of the atom profile and laser profile bandwidths. This effective bandwidth is determined by

$$\delta\lambda' = \sqrt{(\delta\lambda_L)^2 + (\delta\lambda_a)^2} \qquad (55)$$

The saturation spectral energy density, $\rho^s_\lambda(\lambda)$ (J/cm^{3}nm^{-1}), is defined as

$$\rho_\lambda^s(\lambda) = \frac{\delta\lambda'\sqrt{\pi}}{\left(1 + \frac{g_1}{g_2}\right)B_{12}\tau 2\sqrt{ln2}} \tag{56}$$

From this the excitation profile halfwidth, $\delta\lambda_{exc}$ (nm), can be evaluated:

$$\delta\lambda_{exc} = \frac{\delta\lambda'}{\sqrt{ln2}}\sqrt{\ln(2 + \frac{\rho_\lambda(\lambda)}{\rho_\lambda^s(\lambda)})} \tag{57}$$

Alternatively, by measuring the excitation profile of an atom as a function of source spectral energy density, the saturation spectral energy density can be evaluated using the above relation, so long as the laser bandwidth, the atom linewidth and the laser power are each accurately known.

Fluorescence Dip Spectroscopy

To understand the information that can be obtained from the fluorescence dip, it is necessary to know what factors determine the magnitude of the fluorescence dip. Presently, there is not yet a model that fully describes the fluorescence dip, but a model based on a rate equations approach for time independent and time dependent fluorescence dips has been proposed that can predict the behavior of a simple atom, ion or molecule. This model has been detailed elsewhere [52]. In this section, simple mathematical relationships between the fluorescence dip observed and fundamental properties of the analyte will be presented.

For the sake of simplicity, the treatment of the model will assume an atom with three energy levels, where the only processes that will be considered are those shown in Figure 2. Initially the total atom population density, n_T, is considered to be at rest, that is all the atoms are in the ground state. When the population experiences excitation at λ_{12}, such that the excitation rate is sufficient to overcome all radiative and non-radiative relaxations (i.e., the excitation is saturated), an expression for the relative population densities of level 1 and level 2 can be derived, which are essentially steady state during the laser pulse. As has been shown previously, the relative population densities are directly proportional to the statistical weights of the two levels and each level shares a portion of the total population density according to the ratio of its statistical weight (g-value) to the sum of the statistical weights of the levels involved in the excitation/de-excitation process. The steady state (understood to be saturation conditions) population density of level 2, n_2, is equal to the total population, n_T (understood to be the population of the ground state prior to excitation), multiplied by the ratio of $g_2/(g_1+g_2)$, where g_1 and g_2 are the statistical weights of the two levels 1 and 2, respectively. When the same atom population then experiences excitation at λ_{12} and at λ_{23} simultaneously, such that the radiative excitation rates at both wavelengths are sufficient to overcome the radiative and non-radiative relaxations from both level 2 and level 3 (i.e., both transitions are saturated), the population densities of each of the three levels in the three level system are again each proportional to the respective statistical weight of the level. In the case of a two step excitation, the population density of level 2, n_2, is equal to n_T multiplied by the ratio $g_2/(g_1+g_2+g_3)$ where g_1, g_2 and g_3 are the weights of the three levels.

It is intuitive that for a two step excitation, n_2 is less than for a one step excitation, since in the two step excitation case n_T must be distributed among three levels instead of only two. Under saturation conditions, fluorescence is directly proportional to the population density of the fluorescent level and the LIF emission of level 2 is a direct measurement of n_2. By monitoring the fluorescence for both one step and two step excitation, a dip in the fluorescence is observed which is due to the redistribution of the atom population density.

The maximum steady state (saturation conditions) fluorescence dip, Δ_{max}, can be defined as the difference in the relative population density of level 2, n_2/n_T, for the one step excitation and the two step excitation.

$$\Delta_{max} = \left[\frac{(n_2)^{ss}}{n_T}\right]_{(one\ step)} - \left[\frac{(n_2)^{ss}}{n_T}\right]_{(two\ step)} \qquad (58)$$

The maximum fluorescence dip, Δ_{max}, can be reduced through some simple algebra to a convenient expression solely in terms of the weights of the three levels:

$$\Delta_{max} = \frac{g_2}{(g_1 + g_2)} - \frac{g_2}{(g_1 + g_2 + g_3)} \qquad (59)$$

$$= \frac{g_2 g_3}{(g_1 + g_2)(g_1 + g_2 + g_3)} \tag{60}$$

Another useful parameter is the relative fluorescence dip, Δ':

$$\Delta'_{\max} = \frac{\Delta_{\max}}{\left[\dfrac{(n_2)^{ss}}{n_T}\right]_{(one\ step)}} \tag{61}$$

This parameter indicates relatively how much the two step excitation depletes the one step excitation population density of level 2. It can also be reduced to a simple expression of the statistical weights:

$$\Delta'_{\max} = \frac{g_3}{(g_1 + g_2 + g_3)} \tag{62}$$

The relative fluorescence dip is a valuable parameter because it is independent of the total number of atoms and is unaffected by pre- or post-filter effects.

The expressions shown here are for fluorescence dips measured under saturation conditions. For excitation of λ_{23} at less than the saturation irradiance, the observed dip decreases and can be shown to be directly related to the spectral energy density of excitation for the second step by successively attenuating the second step and plotting the relative dip as a function of the spectral energy density. A saturation curve for the second excitation transition is produced which reveals parameters of the excited state transition including the saturation spectral energy density, which is defined as the spectral energy density at which the relative dip is equal to one half of the maximum relative dip. The saturation spectral energy density can be used to calculate the quantum efficiency, Y_{32}, from the equation

$$\rho_\nu^s(\nu_{23}) = \left[\frac{(g_1 + g_2)}{(g_1 + g_2 + g_3)}\right]\left[\frac{8\pi h\nu^3}{c^3}\right]\frac{1}{Y_{32}} \tag{63}$$

A plot of the inverse of the relative dip against the inverse of the spectral energy density shows a linear relationship, the slope of which can be used to determine the quantum efficiency (equation 64):

$$\frac{1}{\Delta'} = \left[\frac{8\pi h\nu^3}{c^3}\right]\frac{(g_1 + g_2)}{g_3}\left[\frac{1}{\rho_\nu(\nu_{23})Y_{32}}\right] + \left[\frac{(g_1 + g_2 + g_3)}{g_3}\right] \tag{64}$$

The relative fluorescence dip can also be used to determine the Einstein absorption coefficient of the second excitation by numerically evaluating equation (65):

$$\Delta'(t) = 1 - \frac{\left[1 - \exp\left(-\left(\frac{g_2}{(g_1 + g_2)}\right)B_{23}\rho_\nu(\nu_{23})\Delta t\right)\right]}{\left[\left(\frac{g_2}{g_1 + g_2}\right)B_{23}\rho_\nu(\nu_{23})\Delta t\right]} \tag{65}$$

From this relationship, B_{23} can be determined which is used to calculate the absorption oscillator strength [53], f_{23}:

$$f_{23} = \frac{4\varepsilon_o m_e h}{e^2}\nu_{23}B_{23} \tag{66}$$

The Einstein coefficient for spontaneous emission can also be evaluated from B_{23}:

$$A_{32} = \left(\frac{g_2}{g_3}\right)\left(\frac{8\pi h\nu^3}{c^3}\right)B_{23} \tag{67}$$

CHAPTER 4
EXPERIMENTAL

Instrumentation

Shown in Figure 3 is a block diagram of the instrumentation used in this experiment. A xenon chloride excimer laser (LPX-110i, Lambda Physik, Gottingen, FRG) was used to pump one of two dye lasers in the one step experiments and both lasers simultaneously in the two step experiments (EPD-330, Lumonics Inc., Kanata, Ontario, Canada, and Model DL-II, Molectron Corp., Sunnyvale, CA). Laser dyes used in this experiment were purchased from Exciton Inc. (Dayton, Ohio) and were prepared according to the laser manufacturer's specifications using pure solvents purchased from Fisher Scientific (Fair Lawn, NJ) and American Burdick and Jackson (Muskegon, MI). Ultraviolet laser radiation was generated for some of the studies by frequency doubling techniques using various nonlinear optical materials. Separation of the fundamental frequency from the doubled outputs was done by using UG-5 and UG-11 Schott glass filters (Corion Corp., Holliston, MA). For the diagnostic studies, it was necessary to attenuate the laser beams systematically. This was accomplished by placing calibrated quartz neutral density filters (Corion Corp., Holliston, MA) in the laser beam path at the dye laser output prior to entrance into the ICP.

Figure 3. Block diagram of experimental setup.

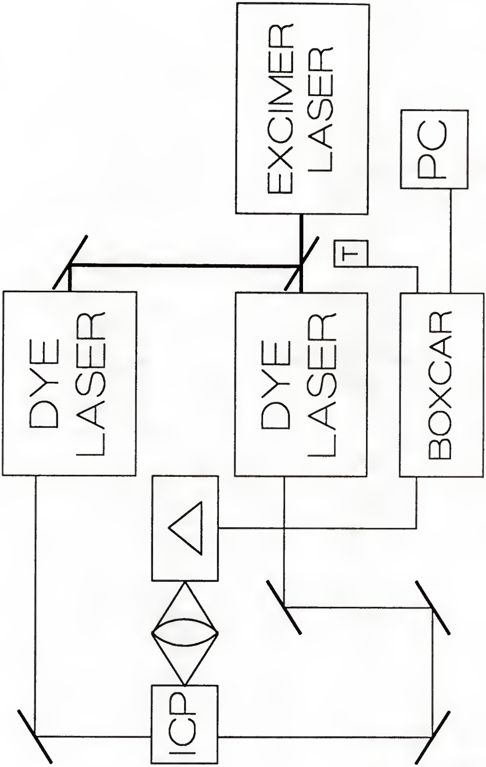
EXCIMER LASER
PC
T
DYE LASER
DYE LASER
BOXCAR
ICP

Laser radiation from the dye lasers was transmitted by quartz prisms to an ICP (Plasma-Therm Inc., Kresson, NJ) that was contained in a laboratory constructed ICP housing designed for laser induced fluorescence studies. The ICP was powered by a 27 MHz radio frequency generator (HFP 2500D, Plasma-Therm Inc., Kresson, NJ) and sustained by a 3 turn coil electrode on a standard quartz torch. Argon gas flows in the ICP were typically 17 L/min for the plasma support gas and 1 L/min for the auxiliary gas. A concentric nebulizer (Model TR-30-A3, J.E. Meinhard and Associates, Santa Ana, CA) was used for sample nebulization and had an argon flow rate of 0.45 L/min. ICP forward powers ranged from 500 W to 1500 W with reflected powers less than 50 W. The observation heights were adjusted for optimum signal to noise ratios for each element studied and ranged from 10 to 30 mm above the load coil. Fluorescence emission from the ICP was collected perpendicular to the laser excitation, imaged with slight magnification onto the slit of a monochromator (Model EU-700, Heath Corp., Benton Harbor, MI) and was detected by a photomultiplier tube (PMT) (R955, Hamamatsu Corp., Middlesex, NJ) which was biased at -900 V and was placed at the exit slit of the monochromator. For intense fluorescence emission signals at high concentrations of analyte, the linear response range of the detector was extended by placing calibrated neutral density filters in front of the monochromator entrance slit.

For each element, the optimum slit width was determined with respect to the signal to noise ratio observed. The PMT anode was terminated into a voltage by a 1000 Ohm load resistor for the analytical studies and a 50 Ohm resistor for the diagnostic studies. The output voltage of the PMT load was connected to the input of a pre-amplifier (Model 4163, Evans Associates, Berkeley, CA) with a gain ten before entering a boxcar averager (SR250, Stanford Research Systems, Palo Alto, CA) that was triggered externally by a photodiode (FND-100, EG&G, Salem, MA) which monitored the output of the excimer laser. The boxcar gate was adjusted, for the analytical studies, to optimize the observation of the pulsed laser induced fluorescence emission signals in the ICP while discriminating against the background emission.

Precise synchronization of the fluorescence pulses with the boxcar gate was insured by adjusting the timing delay of the gate on the boxcar itself and observing their temporal coincidence on an oscilloscope (Tektronix 2430A, Tektronix Inc., Beaverton, OR). The width of the gate (30 ns) was also optimized with respect to the signal to noise ratio of the fluorescence signals for the analytical studies. For the two beam experiments, precise synchronization of the two laser pulses was required for optimum signals to be observed. This was insured by placing a small prism as a scattering element in the sample region of the ICP and detecting the scattered laser radiation with a fast photodiode (200 ps risetime, ET2000, Electro-Optics Technology, Fremont, CA) whose output was connected to the input of an oscilloscope for observation. The beam path of one of the dye lasers to the ICP was then altered by adjustment of a variable beam delay until the timing of the two pulses was matched on the oscilloscope.

For the analytical studies, the boxcar integrator typically averaged 100 laser pulses and the averaged output was sent to a laboratory constructed 1 Hz low pass noise filter. The filtered output was connected to an analog to digital converter computer interface for data acquisition by a personal computer (IBM PC-XT, IBM Inc., Boca Raton, FL) using commercial software (Stanford Research Systems, Palo Alto, CA). For the diagnostic studies, the only changes to the experimental system that were necessary were to use a smaller load on the PMT (50 Ohms) and to shorten the boxcar gate (6 ns). This was done to minimize the distortion of the fluorescence pulse and to provide a more accurate representation of the peak saturated fluorescence signal.

Solutions

Standard stock solutions for copper, silver, gold, lead, scandium, platinum, palladium and iridium were all purchased from commercial suppliers, either Aldrich Chemical Co. (Milwaukee, WI), Fisher Scientific Co. (Fair Lawn, NJ) or Inorganic Ventures (Brick, NJ). Standard stock solutions for dysprosium, cerium, erbium, gadolinium and samarium were prepared by dissolving the appropriate amount of the rare earth oxide (Spex Industries, Metuchen, NJ) in 5 to 10 ml of hot hydrochloric acid and then diluting with distilled deionized water to prepare a 1000 ppm solution of the element. Serial dilution of the stock solutions with distilled deionized water was used to prepare calibration standards which were used to evaluate the sensitivities for each of the elements by ICP-LIF. For the diagnostic studies, a single solution that provided a sufficiently high signal to noise ratio was used for all the measurements of a single element.

CHAPTER 5
ICP-LIF OF RARE EARTH ELEMENTS

Introduction

Rare earth elements are important for geological studies of the earth's crust and for geochemical studies of petrogenesis. There is also significant interest in many of the rare earth elements for industrial research applications such as superconductors. Elemental analysis of the rare earths has been performed by neutron activation analysis, X ray fluorescence [54], and mass spectrometry but is most commonly performed by ICP emission spectrometry (ICP-ES) [55-59], which is very effective because of its high sensitivity, high reproducibility and relative simplicity. Unfortunately, the rare earths have complex emission spectra which produce many spectral interferences and limit the effectiveness of the technique for samples containing mixtures of rare earth elements. The high probability of spectral interferences in combination with a low natural abundance for the rare earths in real samples presents the analyst with many problems in the accurate determination of most of these elements. Much attention has been given to the problem of interferences of the rare earths and many of the proposed solutions have focussed on extensive sample clean up and treatment methods such as ion exchange chromatography prior to analysis. The procedures are often laborious, time consuming and reduce but do not always eliminate the interferences. One solution to this problem is to prepare artificial sample matrices that are free of analyte to determine the effects of the interferences on the analyte signal prior to actual analysis of the sample. Obviously this procedure requires some knowledge of the sample which effectively means that the sample must be analyzed twice, once to determine the interferences and once to determine the analyte.

Recently a rigorous approach has been taken towards the problem of spectral interferences of rare earth elements in ICP-ES. A comprehensive compilation of analyte sensitivities for six of the most common rare earths (Ce, La, Nd, Pr, Sm and Yb) at thirty of their prominent emission lines, as well as "partial sensitivities" of all other rare earths and background equivalent concentrations for a typical ICP emission spectrometer has been reported [46,60,61]. To this point, there has not been a reliable source of information for determining the relative contribution of the various interferences. The systematic study of the interferences and tabulation of the results will enable other scientists to accurately predict interferences based on this data and choose accordingly the optimum emission line for their analysis. While there are sample preparation procedures that can be used to improve the accuracy of ICP-ES determinations and the compilation of the rare earth element emission sensitivities at selected wavelengths will better assist the analyst in "rational line selection", the reason that the spectral interferences in ICP-ES require so much attention is that fundamentally the technique lacks the selectivity to perform trace level determinations of rare earths in samples comprised of rare earth mixtures.

LIF has been used previously to determine rare earth elements in flames [62]. The sensitivity of this method is not competitive with ICP-ES, primarily because of the use of flame atomization. In addition, measurements in this earlier study were limited to the atomic species. In the current study, ICP-LIF is demonstrated as a method that possesses both high sensitivity and high selectivity and is well suited for trace level determinations of rare earth elements, specifically Ce, Dy, Er, Gd and Sm. The use of ICP atomization allows the measurement of ionic species, which are predominant for the rare earth elements in the ICP. This study also demonstrates how LIF using dye laser excitation with a single dye can be used to analyze all these elements and effectively function as a multielement method.

Results

The results of the ICP-LIF analysis of Ce, Dy, Er, Gd and Sm are shown in Table 1 including the wavelengths of excitation and emission. The detection limits reported here, which correspond to the concentration equal to three times the standard deviation of the background signal, are presently the best ever reported for these rare earth elements using LIF in any atomizer [63-65]. The ICP-LIF detection limits compare well with typical ICP-ES detection limits. Two ICP-ES detection limits are shown for three of the elements. The second detection limit corresponds to the ICP-ES detection limit obtained for the element at the wavelength that was used for excitation of the fluorescence in this experiment [3]. This is done to emphasize that the LIF detection limits determined are not necessarily the best

Table 1

Detection limits for 5 rare earth elements by ICP-LIF and ICP-ES

ELEMENT	λ_{exc} (nm)	λ_{fl} (nm)	ICP-LIF (ng/ml)	ICP-ES[a] (ng/ml)	ICP-ES[b] (ng/ml)
Ce	365.585	413.765	30	40	-
Dy	364.541	353.852	15	4	23
Er	363.364	369.264	15	3	-
Gd	364.619	354.580	8	4	30
Sm	363.429	373.598	17	8	66

a. Thermo Jarrell Ash commercial literature, 1987 [66].
b. R.K. Winge et al., Appl. Spectrosc. 33, 206, 1979 [3].

detection limits possible, even though they are currently the best reported. The dynamic ranges were observed to extend from the detection limit to approximately 100 ppm for each of the five elements. For each of the determinations, the limiting noise was the ICP background emission.

One of the purposes of this study was to constrain the possible wavelengths of excitation to a narrow region and to demonstrate the "multielement" capabilities of ICP-LIF using a single laser dye. It is important to emphasize that all of these elements were analyzed using a single laser dye because usually when performing LIF, it is frequently necessary to change dyes when changing analytes. As Table 1 shows, all of these elements were excited in the 360-370 nm region of the spectrum where all were found to have strong absorptions, either from the ground state or from a relatively low excited state that contained a significant portion of the ion population in the ICP.

The use of a single laser dye is important primarily for two reasons. First, by limiting the system to a single dye, the excitation wavelengths obtainable are certainly reduced but the complexity of the experimental system and the overall method are also greatly reduced. LIF is often criticized for being too complex, too specialized and limited to single element determinations. By simplifying the required operation procedures, ICP-LIF can be argued convincingly as being generally useful. Second, by using a single dye to measure five rare earth elements, ICP-LIF can also be argued as a "quasi" multielement method of analysis. The sensitivity of ICP-LIF in this case is just as good as ICP-ES but the selectivity is much improved by using ICP-

LIF. As this study has demonstrated, this is not necessarily true and LIF can in certain analytical applications be developed as a multielement method without major sacrifices of sensitivity, selectivity or analysis time.

The rare earths as a group are characterized by rich emission spectra with many spectral lines in the region from 300-500 nm. The laser induced fluorescence emission of the five rare earths observed in this study were also complex, with fluorescence emission occurring at several different wavelengths simultaneously. These elements are well known for their complex electronic structure which in turn is responsible for their complex emission spectra. The close proximity of the many energy levels of the ions causes extensive collisional coupling and mixing of the excited state populations which gives rise to the large number of fluorescence emission lines observed when a single excitation line is used. The frequent overlap of the emission lines is what causes so many of the spectral interference problems associated with these elements.

In LIF, multiple fluorescence emission lines do not usually cause any significant degradation in selectivity, since any spectral interference would have to absorb the excitation and emit fluorescence at the observed emission wavelength which is unlikely. On the other hand, the mixing of the levels is a problem for LIF because it distributes the population among several levels that are energetically very close. The quantum efficiency of fluorescence, Y_{21}, is greatly reduced as the number of radiative and non-radiative relaxations from the excited state increases [67]. For the rare earths, the mixing of several levels in the excited state creates many alternative routes of relaxation and lowers the quantum efficiency of fluorescence from any one level. The result is that instead of observing intense fluorescence emission at a few emission wavelengths, these elements produce moderately intense fluorescence at many wavelengths and weak fluorescence at even more wavelengths. The lowered quantum efficiency may limit the sensitivity by reducing the fluorescence at a single wavelength, but by distributing the fluorescence emission over many different wavelengths, the selectivity is increased which allows easier qualitative identification. Potentially, the simultaneous detection of several moderately intense emission lines could lead to increased sensitivities by increasing the total fluorescence emission collected.

Spectral Interferences

Another purpose of this study was to demonstrate the need for enhanced selectivity of analysis of the rare earth elements. To do this, a simple interference study of the rare earths by ICP-LIF was performed. Two elements, gadolinium and dysprosium, were chosen as a typical spectral interference that might occur for two rare earths. In this study, dysprosium was considered to be the analyte and gadolinium was the interferant. Dysprosium ion has a strong absorption line at 364.541 nm and a strong fluorescence emission line at 353.170 nm. Gadolinium ion has two absorptions very close to the dysprosium absorption at 364.562 nm and at 364.619 nm. Gadolinium ion also has a strong collisionally assisted fluorescence emission at 352.854 nm. Shown in Figures 4 and 5 are partial energy level diagrams for dysprosium and gadolinium.

Accurate measurements of these two elements in this wavelength region (364 nm) would be virtually impossible by ICP-ES because of the small wavelength separation of the two absorption/emission lines [68]. Unfortunately, this is exactly the type of experimental situation that often occurs in multielement rare earth determinations. While the higher selectivity of ICP-LIF can greatly improve the accuracy of the measurement, it is not always sufficient. Shown in Figures 6 and 7 are fluorescence excitation scans of a dysprosium solution and a solution containing both dysprosium and gadolinium, respectively. The wavelength of excitation is scanned from approximately 364.3 nm to 365.0 nm, and the fluorescence is observed at 353.170 nm. As the ICP-LIF excitation scans show, there is a considerable amount of background emission noise generated by both of these elements at the fluorescence emission wavelength. For samples containing several interfering species, the background emission could possibly drown out the analyte fluorescence emission.

For these two elements, wing excitation is very important. Since the analyte and the interferant each have a strong absorption line very close to each other, there is a strong probability that the excitation profiles of the analyte and the interferant will be broadened by high power laser excitation (saturation broadening). This broadening can actually cause spectral interferences that would not normally occur for lower power sources and is not a consideration except for very small wavelength differences and high laser powers. In the case of dysprosium and gadolinium, the

Figure 4. Partial energy level diagram of Dy II.

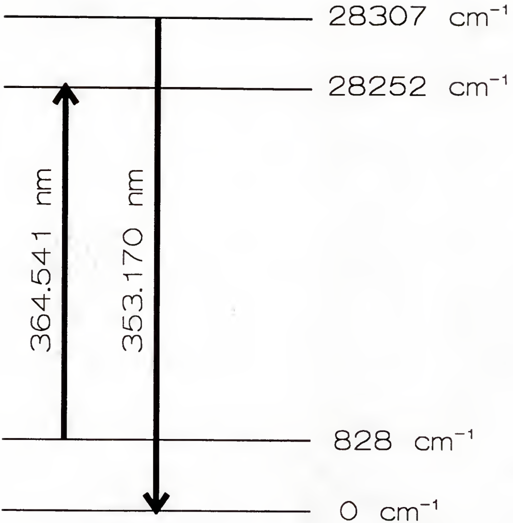
28307 cm⁻¹
28252 cm⁻¹
828 cm⁻¹
0 cm⁻¹
364.541 nm
353.170 nm

Figure 5. Partial energy level diagram of Gd II.

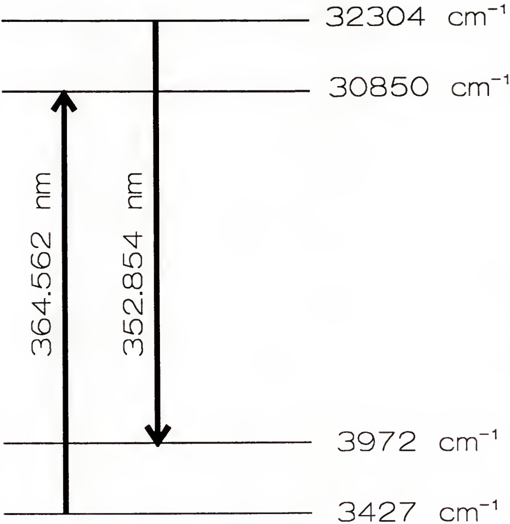
32304 cm⁻¹
30850 cm⁻¹
364.562 nm
352.854 nm
3972 cm⁻¹
3427 cm⁻¹

Figure 6. Fluorescence excitation scan of 10 ppm Dy II

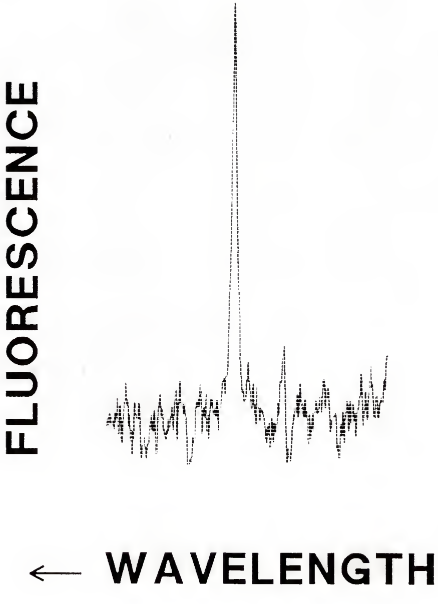
FLUORESCENCE
← WAVELENGTH

Figure 7. Fluorescence excitation scan of 10 ppm Dy II + 500 ppm Gd II.

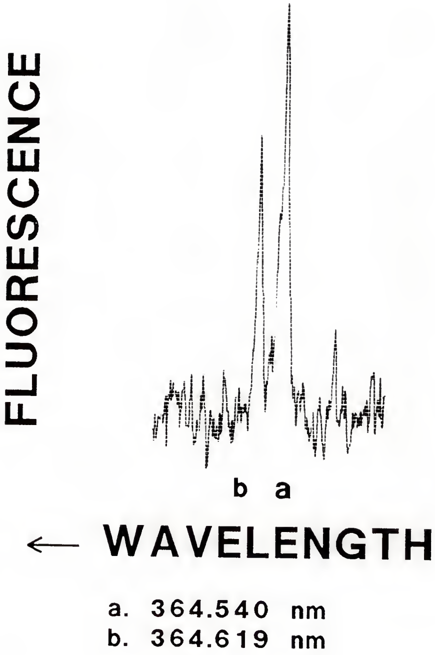
FLUORESCENCE
b
a
← WAVELENGTH
a. 364.540 nm
b. 364.619 nm

wavelength separation is so small that any broadening of the excitation profiles will cause a significant amount of spectral overlap. Under normal circumstances, even if the excitation profiles overlap, the fluorescence emission can be observed in a region free of spectral overlaps. However, if the fluorescence emission of analyte and the interferant also overlap, a spectral interference can occur in ICP-LIF.

By measuring the spectral linewidths of the fluorescence excitation profile, it is possible to determine how much the excitation profile is broadened by laser saturation of the excitation transition. The saturation broadening of fluorescence excitation profiles has been studied previously in flames for calcium, strontium, sodium and indium [48,49]. Using a relationship derived from those studies, the excitation profile spectral linewidth can be evaluated to determine the amount of saturation broadening that is occurring in the current study. Based on the dye laser spectral bandwidth which is 0.003 nm and the linewidth of the dysprosium ion in the ICP which has been reported as being 0.0025 nm [69], the unbroadened linewidth of the excitation profile is 0.0039 nm. The absorption rate for laser excitation can be calculated using the following equation with the appropriate experimental parameters:

$$R_{12} = \frac{g_2}{g_1} A_{21} \left(\frac{\lambda^3}{8\pi hc} \right) \left(\frac{Q_L}{\delta t_L \; S_L \; \delta \nu_L} \right) \tag{68}$$

where R_{12} is the rate of excitation between levels 1 and 2 (s^{-1}), g_i is the statistical weight of level i (i=1 or 2), A_{21} is the Einstein coefficient for spontaneous emission (s^{-1}), λ_{12} is the wavelength of the transition between the two levels (nm), h is Planck's constant (Js), c is the speed of light (m/s), Q is the pulse energy of the laser (J), t_L

is the pulse duration of the laser (s), S_L is the cross section of the laser beam (m^2) and $\delta\nu_L$ is the frequency bandwidth of the laser (Hz). Assuming that the transition rate saturates at 10^9 transitions per second, it is estimated that the laser excitation is saturating the excitation by about 10^3 to 10^4 times. Using the calculated saturation value, the observed excitation profile should be broadened to about 0.0123 nm. The experimentally observed halfwidth of the dysprosium ion excitation profile is about 0.0156 nm FWHM, which is in fair agreement and suggests that the high laser power is responsible for the broadened excitation profile.

Shown in Table 2 are the results of the study that demonstrates a spectral interference occurring as a result of saturation broadening for dysprosium and gadolinium ions. The effects of the broadened profiles becomes evident for the solution containing both dysprosium and gadolinium. The experimentally determined linewidths for the dysprosium solution alone shows that the excitation profile of the ion is broadened by the high laser powers. Using the experimentally determined linewidth and the laser energy density output, the saturation spectral energy density of the dysprosium absorption transition can be determined using equation 57 which was derived previously. The experimentally determined saturation spectral energy density of this transition is approximately 8.9×10^{-14} J/m^3Hz.

$$\rho_\nu^s(\nu) = \rho_\nu(\nu)\ \exp(-\left(\frac{\delta\lambda_{exc}}{\delta\lambda'}\right)^2 \cdot ln2\ ) \tag{69}$$

Table 2

Excitation profile linewidths for Dy and Gd as a function of laser spectral energy density

ELEMENT	FWHM_{obs} (pm)	FWHM_{calc} (pm)
Dy 10 ppm	15.6	3.9
Dy 10 ppm + Gd 500 ppm	28.5	-
Dy 10 ppm + Gd 500 ppm (0.7)[a]	14.7	14.4
Dy 10 ppm + Gd 500 ppm (1.0)[a]	14.7	13.8
Dy 10 ppm + Gd 500 ppm (2.0)[a]	12.0	11.9

a. Numbers in parentheses refer to the value of neutral density filter used to attenuate the laser beam.

It is also estimated from equation 69 that the excitation is saturated by over 6×10^4 times.

As already stated, gadolinium ion has a strong absorption line which is very close to the dysprosium absorption line ($\Delta\lambda < 0.020$ nm). Sufficiently high laser powers at the dysprosium absorption wavelength partially excite the gadolinium absorption simultaneously. Gadolinium ion also has a fluorescence emission line which is close to the dysprosium fluorescence emission line. The two lines are only separated by 0.316 nm, and both are well within the spectrometer bandpass for these measurements (1 nm bandpass for a 500 μm slit width). As the experimentally determined linewidths show, the solution containing a mixture of 10 ppm dysprosium and 500 ppm gadolinium shows a significantly broader linewidth than the solution containing dysprosium alone. At high laser powers, the observed profile linewidth is nearly doubled from 15.6 pm to 28.5 pm due to wing excitation of the gadolinium ion interferant.

The major problem with such a spectral interference is that even by using a narrow linewidth dye laser to hopefully resolve the analyte and interferant species, high laser powers can broaden the excitation profiles of the two species and cause them to overlap which obviously degrades the selectivity of the fluorescence measurement. The observed fluorescence emission using high powered excitation may have contributions from both the analyte and the interferant. Spectral interferences due to saturation broadening can be avoided, however, by decreasing the laser power to narrow the excitation profiles and reduce the amount of spectral overlap of the profiles. This reduction of the spectral interferences is shown by the decreasing values of the profile linewidths observed for successive attenuations of the laser power using neutral density filters. By reducing the laser power ten times, the linewidth is narrowed by almost 50 % to 14.7 pm. By reducing the laser power a hundred times, the linewidth is reduced to 12.0 pm. Based on the degree of saturation determined by the linewidth measurement of dysprosium ion alone, the profile linewidths for reduced powers of dysprosium ion can be predicted. These values are shown as theoretical values in comparison to the observed linewidths of the dysprosium and gadolinium mixture. The significance of the comparison is clear. As the laser power is reduced the observed linewidths of the mixture quickly approach the predicted linewidths of the pure dysprosium profile linewidths. Decreasing laser powers, while still being sufficient to saturate but insufficient to broaden the excitation profile, can be used to maintain the high selectivity of the ICP-LIF method without sacrificing the sensitivity.

Therefore, for ICP-LIF determinations of elements where there is a strong possibility of spectral interferences at both the excitation and emission wavelengths, serious consideration must be given to saturation broadening of the absorption profile, which can cause inaccuracies. This is especially important for rare earth elements, in particular cerium, gadolinium and lanthanum, which all have very rich and complex spectra. Further investigations are needed to ultimately determine the relative importance of this effect on the performance of ICP-LIF.

CHAPTER 6
SINGLE AND DOUBLE RESONANCE ICP-LIF

Introduction

The vast majority of ICP-LIF studies reported are performed by single resonance or single step excitation, that is, a single dye laser tuned to an atomic or ionic transition is used to excite the analyte species of interest from a low lying level, at or close to the ground state, to an excited state that is generally a few eV (2 to 4 eV) above the ground state [63,70-72]. Fluorescence emission is observed from the excited state either at the same wavelength, or if possible at a wavelength different from the excitation wavelength. Not much attention has been given to the possibility of using a second dye laser to doubly excite atoms and ions. By simultaneously exciting the analyte species excited by the first laser to higher levels, fluorescence emission of these highly excited species can be observed [29,45,64,73]. Double resonance excitation, or two-step excitation as it is often referred to, allows atoms and ions to be excited to levels several eV above the ground state which normally cannot be reached in a single excitation step.

From an analytical standpoint, there are reasons for performing double resonance excited ICP-LIF that are potentially advantageous over single resonance fluorescence. First, transitions from high lying levels often have large oscillator strengths which enhances the detection of fluorescence emission from those levels. Second, these transitions are often very energetic transitions and the fluorescence emission wavelengths tend toward the ultraviolet region of the spectrum. This can also enhance fluorescence detection since the ultraviolet region is a relatively low noise region for the ICP. Potentially there is a drawback in sensitivity for double resonance methods since the laser induced population of a level is reduced for double resonance excitation compared to single resonance excitation because the atom or ion population is distributed over three or more levels instead of two. Despite the reduced population, there is no significant loss in sensitivity for double resonance fluorescence relative to single resonance fluorescence provided that both of the excitation transition wavelengths are saturated for the two steps and a fluorescence emission wavelength is chosen which has a high transition probability (or large oscillator strength) for spontaneous emission [73,74].

Other analytical advantages of double resonance fluorescence include easy scatter correction and no post filter or self reversal effects, both of which are major concerns for single resonance fluorescence when the excitation wavelength is within the bandpass of the spectrometer used for detection. Scatter correction in double resonance excited resonance fluorescence can be performed simply by measuring the signal obtained when both excitation wavelengths are present, which represents the combined two-step fluorescence and scatter signals, and when only the second step excitation wavelength is present, which represents the scatter signal alone. The true double resonance fluorescence signal is simply the difference between the two measured signals.

The absence of post filter effects in double resonance fluorescence can be attributed to the fact that the fluorescence emissions induced by two-step excitation are excited state transitions that usually terminate at levels well above the ground state. Even at ICP temperatures (4000-6000°K), the populations of these levels is negligible, which precludes any reabsorption of the fluorescence emission by analyte atoms outside the probe region of the laser.

However, the unique advantage of double resonance fluorescence is the outstanding selectivity that is achieved using dual dye laser excitation. While laser induced single resonance fluorescence is well recognized for having high selectivity, the addition of a second dye laser improves the overall selectivity dramatically. The use of narrow linewidth lasers guarantees highly selective excitation of the analyte species and by using two lasers to doubly excite the analyte, spectral interferences that might occur after one excitation are eliminated by a second excitation. In practice, double resonance fluorescence of atoms and ions can claim virtual freedom from spectral interferences and approaches elemental specificity.

Copper, silver, lead, gold, platinum, palladium and scandium have each been determined by ICP-LIF using single resonance and double resonance excitation schemes. The results are shown for the purposes of direct comparison of the analytical figures of merit of the two types of excitation. The results are also presented to demonstrate the unique ability of double resonance ICP-LIF to combine high sensitivity with extremely high selectivity. The results of silver and lead determinations for a standard reference material (NBS-SRM 498, copper alloy) using single resonance and double resonance ICP-LIF are also presented to demonstrate the usefulness of the technique(s) for analysis of real samples.

Silver

The single resonance fluorescence of silver atom was performed by exciting from 0 to 30473 cm^{-1} using the resonance transition at 328.068 nm (Fig. 8). Intense fluorescence emission from 29552 to 0 cm^{-1} was observed at 3382.89 A. For the double resonance fluorescence, silver was also excited at 328.068 nm for the first step with simultaneous excitation of the second step from 30473 to 48764 cm^{-1} at 546.549 nm. Collisionally assisted fluorescence from 48744 to 29552 cm^{-1} was then observed at 520.907 nm. The two step excited fluorescence was also very intense indicating the stepwise excitation was highly efficient which is expected when the two excitation transitions are directly coupled through a common level.

The results of the single resonance and double resonance studies are shown in Table 3. The detection limits are shown in comparison to the best ICP-AFS detection limits reported to date. It is worth mentioning that in the cases of copper, gold, palladium and silver, a desolvation sample introduction technique was used that can improve the overall sensitivity of the method by about one order of magnitude. Detection limits comparisons for these elements should consider this difference in the two measurement methods. The detection limits being reported correspond to

Figure 8. Partial energy level diagram of Ag.

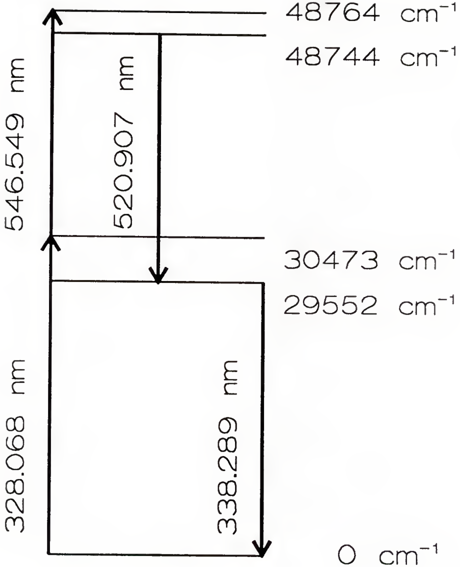
48764 cm⁻¹
48744 cm⁻¹
546.549 nm
520.907 nm
30473 cm⁻¹
29552 cm⁻¹
328.068 nm
338.289 nm
0 cm⁻¹

Table 3

Detection limits for 7 elements by ICP-LIF and ICP-AFS

ELEMENT	SINGLE RESONANCE (ng/ml)	DOUBLE RESONANCE (ng/ml)	ICP-AFS (ng/ml)
COPPER	2.7	6.9	0.2[a]
SILVER	0.8	1.7	<0.1[a]
GOLD	4.2	6.0	0.3[a]
PLATINUM	3.3	29	4[b]
PALLADIUM	3.9	45	2[a]
LEAD	0.7	30	1[c]
SCANDIUM	0.2	13	30[d]

a. D.R. Demers, Amer. Lab. 30, 1987 [38].
b. X. Huang et al., Appl. Spectrosc. 39, 1042, 1985 [72].
c. N. Omenetto et al., Spectrochim. Acta 39B, 115, 1984 [70].
d. M.A. Kosinski et al., Talanta 30, 339, 1983 [75].

the concentration that produces a signal equal to three times the standard deviation of the measured blank signals. The detection limits of silver by single resonance and double resonance ICP-LIF are very similar and the dynamic ranges of the two techniques extend to at least 100 ppm. The overall sensitivities for both techniques are very good and are very similar which indicates that there are few extra losses in the double resonance fluorescence of silver in comparison to the single resonance.

Gold

The single resonance fluorescence of gold atom was performed by using a resonance fluorescence scheme (the excitation and emission wavelengths are the same) by exciting at 267.595 nm which excites the gold from 0 to 37359 cm^{-1} (Fig. 9). The double resonance fluorescence also used the 267.595 nm transition as a first step followed by excitation at 406.508 nm from 37359 to 61952 cm^{-1}. The double resonance fluorescence of gold was observed from the collisionally coupled level at 62034 cm^{-1} to 41174 cm^{-1} at 479.260 nm. As in the case of silver, intense two step excited fluorescence was observed suggesting very efficient population of the upper level of gold.

The strong fluorescence emission produced by both the single and double resonance excitation schemes of gold provided very good sensitivity for both the techniques. Unlike silver, the gold fluorescence studies showed a significant difference in the dynamic ranges for the single and double resonance excitations. The single resonance fluorescence of gold became nonlinear above 10 ppm which

Figure 9. Partial energy level diagram of Au.

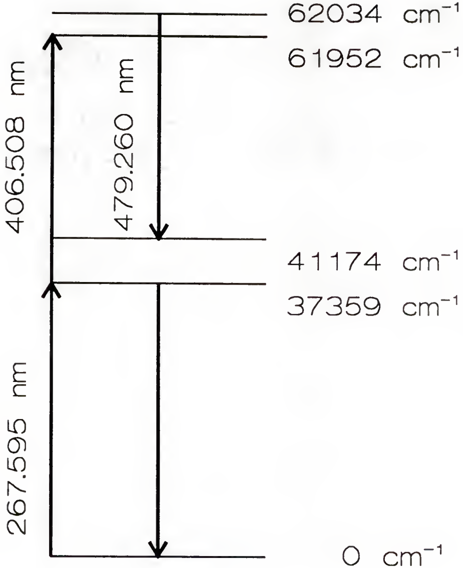
62034 cm⁻¹
61952 cm⁻¹
41174 cm⁻¹
37359 cm⁻¹
0 cm⁻¹
406.508 nm
479.260 nm
267.595 nm

limits the dynamic range to about 4 orders of magnitude. This nonlinearity is presumed to be due to post filter or self reversal effects by gold atoms outside the laser probe region in the ICP and has been reported previously [72]. The double resonance fluorescence on the other hand does not show such nonlinearity at higher concentrations. The double resonance fluorescence emission occurs from highly excited states to lower lying excited states. The population in these lower excited states is negligible in the ICP, and it is unlikely that the double resonance fluorescence emission would be attenuated by reabsorption. The dynamic range of the double resonance technique is extended relative to the single resonance technique to about 6 orders of magnitude. Therefore, the double resonance fluorescence has similar sensitivity as the single resonance at concentrations approaching the detection limit but in this case significantly improves the LDR at higher concentrations and certainly has higher selectivity than the single resonance fluorescence technique.

Platinum

The single resonance fluorescence of platinum atom was performed by exciting platinum from 0 to 37591 cm^{-1} at 265.945 nm and observing fluorescence emission at 271.904 nm from 37591 to 824 cm^{-1} (Fig. 10). The double resonance fluorescence also proceeded by way of an initial excitation at 265.945 nm. These singly excited atoms were simultaneously excited at 449.845 nm and the resulting fluorescence emission was observed at 390.073 nm from 59751 to 34122 cm^{-1}. The results of the

Figure 10. Partial energy level diagram of Pt.

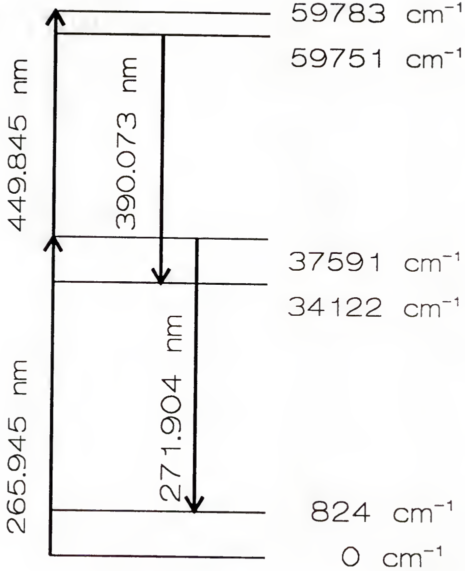
59783 cm^{-1}
59751 cm^{-1}
449.845 nm
390.073 nm
37591 cm^{-1}
34122 cm^{-1}
265.945 nm
271.904 nm
824 cm^{-1}
0 cm^{-1}

single and double resonance fluorescence studies of platinum show that, unlike silver and gold where the relative sensitivities of the single and double resonance techniques are very similar, the platinum detection limit for the double resonance is about one order of magnitude worse than that of the single resonance. The most likely reason for the difference in the detection limits is the collisional coupling or mixing of platinum levels in the ICP. The first and second excited states that are achieved in the double resonance excitation of platinum are each part of a large manifold of several excited states. Within these manifolds, the levels are all separated by relatively small energy differences (<1000 cm^{-1}). When a platinum atom is optically pumped into one of the excited states in the manifold and suffers a collision, the probability that one of the nearby levels in the manifold will be populated increases as the energy separation between the two levels decreases [76]. For platinum, the large number of levels in the excited state greatly enhances the probability that collisional coupling will occur. Collisional coupling depopulates the desired level and lowers the quantum efficiency of the observed fluorescence from that level. This depression of the quantum efficiency of fluorescence in ICP-LIF has been studied and reported previously by Uchida et al. [67]. For double resonance fluorescence, the effects of this coupling are multiplicative since this coupling can occur at both the intermediate and upper levels reached during the two excitation steps. Therefore, the results of this coupling are more obvious for the double resonance fluorescence than the single resonance.

Other evidence of collisional coupling is that fluorescence is observed from levels other than the one achieved in the absorption. For both the single and double resonance fluorescence of platinum, the fluorescence emission spectra are characterized by many emission lines that correspond to transitions occurring from coupled levels. This is easily verified for the double resonance excitation of platinum by performing a fluorescence excitation scan. By tuning one laser to the first excitation transition of platinum and keeping this laser and the fluorescence emission monochromator constant while scanning the second laser, a fluorescence excitation profile of the upper excited state can be obtained. This profile indicates specifically which transitions are connected either directly or indirectly through collisions and are capable of promoting platinum from the intermediate level at 37591 cm^{-1} to the excited state whose fluorescence is being monitored. The first laser was tuned to 265.945 nm and the fluorescence monochromator was set at 390.073 nm. The second laser was scanned from 448 nm to 452 nm, a wavelength region that was observed to have a large number of excited state transitions most of which are coupled by collisions. Shown in Figure 11 is a double resonance fluorescence excitation scan for platinum. It is interesting to note that of the seven clearly observable resonances in this scan, only one corresponds to a previously reported transition to the best of our knowledge. Tentative wavelength assignments were made by recording the wavelength reading on the laser when the observed fluorescence was at a maximum and are shown in Table 4. The relative fluorescence emission intensities of the absorption resonances are also included. By calculating the energy differences that

Figure 11. Double-resonance fluorescence excitation scan of Pt.

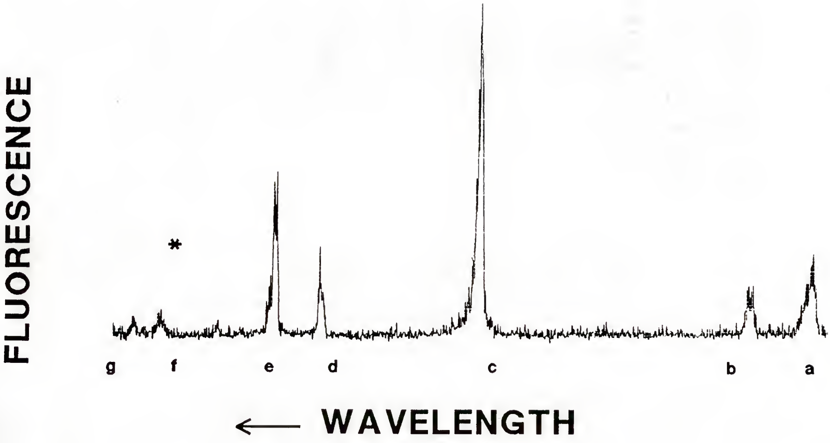
FLUORESCENCE
*
g
f
e
d
c
b
a
← WAVELENGTH

Table 4

Wavelength assignments for 7 resonances observed for a double resonance fluorescence excitation scan of Pt

OBSERVED λ (nm)	Relative Intensity	Energy Levels (cm^{-1})
(a) 448.465	0.51	37591 - 59882
(b) 448.655	0.25	37591 - 59882
(c) 449.845	1.00	37591 - 59783
(d) 450.835	1.00	37591 - 59764
(e) 451.105	0.54	37591 - 59751
(f) 452.090[a]	0.11	37769 - 59882
(g) 452.315	0.09	37769 - 59872

a. This wavelength reported previously in the literature (C.H. Corliss and W.R. Bozman, NBS Monograph 53, 1962 [77]).

these wavelengths correspond to and comparing them to the energy level diagram of platinum, the unreported wavelengths can be roughly correlated to allowed transitions between known levels. However, the scanning of the dye laser, which was performed manually, limits the accuracy and the usefulness of the wavelength assignments. Assuming that the wavelength determination is accurate, the excitation transition that produces the most fluorescence at 390.073 nm is at 449.845 nm.

An interesting result of this double resonance excitation scheme for platinum is the extraordinary selectivity achieved. While collisions are observed to lower the sensitivity of the method by lowering the quantum efficiency of the fluorescence, the fluorescence excitation scan that results from the collisionally coupled populations of other levels can be used as a fingerprint for platinum. There is virtually no possibility of spectral interferences in this excitation scan because of the large number of excitation resonances that are characteristic of platinum in this spectral region. The elimination of interferences by performing an excitation scan is a distinct advantage of the double resonance method that separates it from most if not all other methods since very few analytical methods can simultaneously claim both high sensitivity and selectivity which approaches elemental specificity.

Palladium

The single resonance fluorescence of palladium atom was performed by exciting from 6564 to 37394 cm^{-1} at 324.270 nm (Fig. 12). Collisionally assisted fluorescence emission was observed from 35928 to 6564 cm^{-1} at 340.458 nm. The

Figure 12. Partial energy level diagram of Pd.

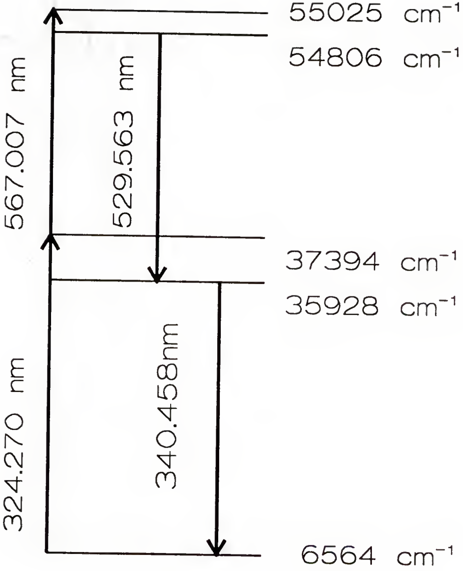
55025 cm⁻¹
54806 cm⁻¹
567.007 nm
529.563 nm
37394 cm⁻¹
35928 cm⁻¹
324.270 nm
340.458nm
6564 cm⁻¹

double resonance fluorescence of palladium also used the single resonance excitation as the first step in the two step excitation with the second step occurring at 567.007 nm from 37394 to 55025 cm^{-1} while the fluorescence emission was observed at 529.563 nm from 54806 to 35928 cm^{-1}. A major difference between the scheme used for palladium and the schemes used for the other three elements is that the first step used for palladium is not a resonance transition; it is not directly connected to the ground state. In fact the lower level in this transition is at 6564 cm^{-1} or about 0.81 eV above the ground state. Despite the high energy of this level, excitation of fluorescence from this excited state proved to be very sensitive for two reasons. First, even at moderate ICP powers, the temperature of the plasma is high enough so that a sizable population accumulates in this level, possibly as high as 20% that of the ground state. In addition, the absorption transition from this level has a large oscillator strength that is much more probable than the resonance transition. These two factors combined make atomic fluorescence in the excited state for palladium very effective.

The analytical results obtained for the single and double resonance fluorescence of palladium are very similar to the platinum results. There is considerable difference in the limits of detection for the single and double resonance fluorescence of palladium which is a result of the collisional coupling of numerous levels to the excited states that are reached directly by the laser excitation, except that the loss in sensitivity is more significant for palladium. However, it is important to note that even though both the platinum and palladium results showed losses in sensitivity when a second excitation step is added, the excitation schemes selected for these elements did not take possible collisional losses into account. Therefore these may not be the best schemes to use for optimum sensitivity. By selecting transitions that include levels that are not as susceptible to collisional couplings, it may be possible to improve upon the sensitivity of the double resonance fluorescence for these two elements.

Copper

The single resonance fluorescence of copper atom was performed by exciting at 324.754 nm from 0 to 30784 cm^{-1} and observing at 327.396 nm from 30535 to 0 cm^{-1} (Fig. 13). The double resonance fluorescence was stepwise excited from 30784 to 49942 cm^{-1} at 521.820 nm and thermally assisted fluorescence was observed at 515.324 nm from 49935 to 30535 cm^{-1}. Both fluorescence excitation schemes produced intense fluorescence emission at the observed wavelengths. The limits of detection are both in the low ppb range and are comparable to each other indicating that there are very few losses in the two step excitation relative to the one step excitation scheme. A large linear dynamic range covering 5-6 orders of magnitude is observed for both the techniques.

Figure 13. Partial energy level diagram of Cu.

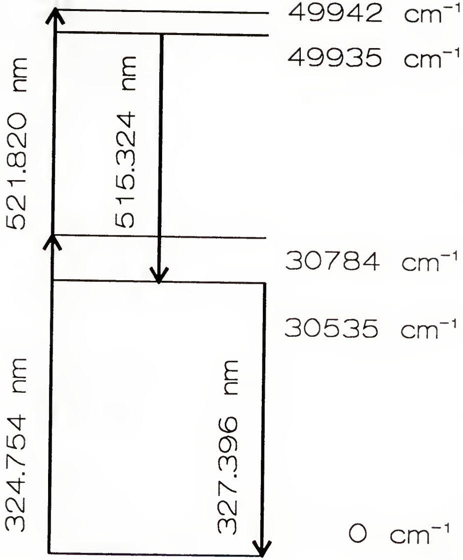
49942 cm^{-1}
49935 cm^{-1}
30784 cm^{-1}
30535 cm^{-1}
0 cm^{-1}
521.820 nm
515.324 nm
324.754 nm
327.396 nm

Lead

The single resonance fluorescence of lead atom was performed by exciting lead at 283.306 nm from 0 to 35287 cm^{-1} and observing direct line fluorescence at 405.783 nm from 35287 to 10650 cm^{-1} (Fig. 14). The double resonance fluorescence was performed by stepwise exciting singly excited lead atoms from 35287 to 51944 cm^{-1} at 600.193 nm and observing thermally assisted fluorescence at 239.379 nm from 52412 to 10650 cm^{-1}. The single resonance fluorescence of lead atom was observed to be much more intense than the double resonance fluorescence emission. The sensitivity of the double resonance fluorescence was also poorer and is reflected in the higher detection limit. Both techniques exhibited good linearity over approximately 5 orders of magnitude.

The great difference in the sensitivities and detection limits for the two techniques is evidently due to the strong relaxation processes to the metastable levels of the lead atom. The relatively long lifetimes of the metastable levels means that any atoms which relax to the levels are effectively "trapped" and are no longer available for fluorescence during the laser pulse [29]. The metastables drain a portion of the singly excited population and trap it for the duration of the laser pulse, which limits the number of atoms available for a second excitation. Those atoms that are excited by the double resonance scheme also can relax to the metastable levels and become trapped. Since these atoms are not recycling, the number of atoms left for fluorescence is quickly depleted and the fluorescence decays rapidly in intensity. Lead atom suffers losses to the metastable levels for both the single

Figure 14. Partial energy level diagram of Pb.

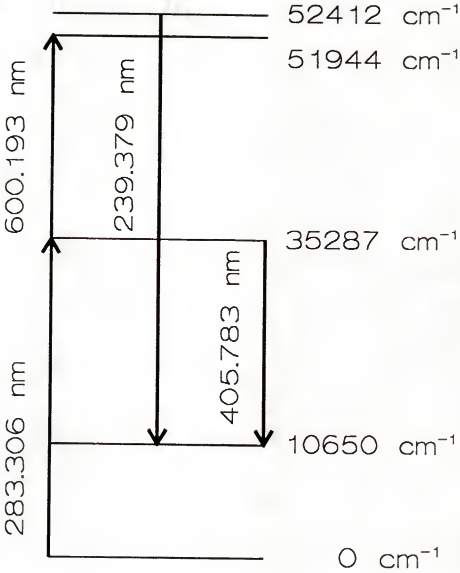
52412 cm^{-1}
51944 cm^{-1}
35287 cm^{-1}
10650 cm^{-1}
0 cm^{-1}
600.193 nm
239.379 nm
405.783 nm
283.306 nm

resonance and the double resonance excitation steps, and it therefore is not surprising that the population depletion at both steps is more significant for the double resonance than for the single resonance fluorescence emission.

Scandium

Single resonance fluorescence of scandium ion was performed by exciting the ion at 361.384 nm from 178 to 27841 cm^{-1} (Fig. 15). The thermally assisted fluorescence emission was observed at 357.4 nm from both 28161 to 178 cm^{-1} and 28021 to 68 cm^{-1}. The double resonance fluorescence was performed using a disconnected scheme. The collisionally coupled population of the singly excited ion was excited at 261.122 nm from 26081 to 64366 cm^{-1} and the thermally assisted fluorescence emission was observed at 303.993 nm from 65236 to 32350 cm^{-1}. The detection limits differ greatly for the two types of excitation. The detection limit for the single resonance fluorescence of scandium ion is exceptional. The superior sensitivity evidently is because of two intense fluorescence emission lines that are spectrally very close to each other which are detected simultaneously. The single resonance fluorescence emission spectrum of scandium ion displays an assortment of emission lines which signify that an extensive redistribution of the excited state population occurs via collisions in the ICP. Usually this type of coupling implies that the observed fluorescence emission will be reduced, due to lowering of the quantum efficiency. This effect has already been observed and discussed previously for several elements, such as the rare earths and platinum and palladium. However, in the case

Figure 15. Partial energy level diagram of Sc II.

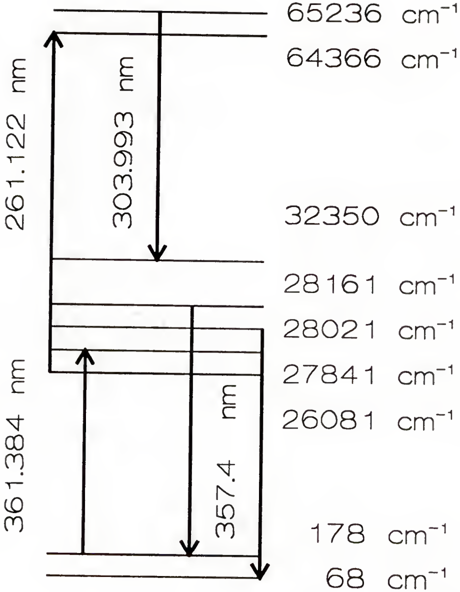
65236 cm⁻¹
64366 cm⁻¹
32350 cm⁻¹
28161 cm⁻¹
28021 cm⁻¹
27841 cm⁻¹
26081 cm⁻¹
178 cm⁻¹
68 cm⁻¹
261.122 nm
303.993 nm
361.384 nm
357.4 nm

of scandium ion, the intense fluorescence emission of the two lines at 357.253 nm and 357.635 nm greatly improves the fluorescence detection, since both emission lines can easily be included in the spectrometer bandpass simultaneously. The statistical weights of the two levels are 7 and 5 which means that by monitoring both lines, the ion population observed is effectively doubled which accounts for the excellent sensitivity.

The double resonance fluorescence of scandium ion is almost two orders of magnitude less sensitive than the single resonance fluorescence but both techniques are characterized by large linear dynamic ranges of over 5 orders of magnitude. The collisional coupling to the laser populated level is also quite extensive for the double resonance excited scandium ion. This coupling reduces the quantum efficiency of fluorescence which lowers the sensitivity of the technique. Although the sensitivity is sacrificed somewhat in double resonance fluorescence of scandium ion, there are unique merits to the technique. The selectivity is of course improved but there is also the opportunity for discovering excited state transitions. In this study, a previously unreported emission wavelength was observed when the double resonance fluorescence emission spectrometer was scanned. The emission wavelength was observed at approximately 297.7 nm and while there is not much information that can be obtained from this, the potential for double resonance to study atomic and ionic excited state transitions needs to be emphasized.

It is important to mention that double resonance ionic fluorescence has been performed as opposed to atomic fluorescence. This technique has tremendous analytical potential in terms of sensitivity since the second ionization potential of most elements is usually so high that ionization losses, which often limit the sensitivity and the scope of excitation wavelengths in atomic double resonance fluorescence, are negligible for the ion. The high sensitivity of ionic ICP-LIF has already been demonstrated for the alkali earth metals but has yet to be fully exploited for other elements [45].

Analysis of a Standard Reference Material

The analysis of a standard reference material was performed as a demonstration of the accuracy of the single resonance fluorescence and double resonance fluorescence techniques. The standard reference material from the National Bureau of Standards was an unalloyed copper sample, NBS-SRM 498, which contained certified ppm levels by weight of several other elements, including lead and silver. The copper sample, prior to dissolution, was etched in a 1 to 1 mixture of ultrapure nitric acid and distilled deionized water (DDW), rinsed with DDW, dried and weighed. After weighing, the sample was partially dissolved in ultrapure nitric acid with gentle heating until approximately 17 g had been dissolved. The undissolved sample was removed, rinsed with DDW to wash any remaining dissolved copper back into the sample solution, and the exact amount of dissolved copper was determined by weighing the undissolved copper. Dilute nitric acid solutions were added to the acid solution containing the dissolved copper and the entire solution was then digested for several hours to insure complete dissolution of the copper.

This sample stock solution was diluted with DDW to produce solutions containing approximately 5% nitric acid and 1 to 2% (weight/volume) of the copper sample, which is roughly the maximum level of salt content in solution that the sample nebulizer will tolerate. Several sample solutions were prepared, three for the silver determinations and four for the lead determinations. For each element, one solution was unaltered and the remaining solutions were spiked with varying amounts of concentrated solutions of the element. The analyte concentrations in the sample were then determined by the method of standard additions using ICP-LIF.

Table 5 shows the results obtained for lead and silver determinations of NBS-SRM 498 by single resonance and double resonance ICP-LIF using the method of standard additions. The agreement of the experimental values with the certified values is excellent. As expected, the higher selectivity of double resonance fluorescence provided better accuracy as well as less uncertainty for the two determinations. Despite intense background copper emission, the high selectivity of single resonance ICP-LIF and the extremely high selectivity of the double resonance ICP-LIF were evident by the high signal to noise ratio observed for the unspiked sample solutions which contained sub-ppm levels of both the elements. In fact, the double resonance fluorescence signal to noise ratio was observed to be nearly identical to the signal to noise ratio of a calibration standard of similar concentration. This is an excellent example of the analytical power of the double resonance fluorescence method. The accuracy of these results demonstrates that ICP-LIF has

Table 5

Results of Ag and Pb determinations of NBS (NIST) SRM 498 by single resonance and double resonance ICP-LIF

	SINGLE RESONANCE (mg/ml)	DOUBLE RESONANCE (mg/ml)	CERTIFIED VALUE (mg/ml)
SILVER	18.7 +/- 1.1	19.6 +/- 0.9	20.1 +/- 0.4
LEAD	10.6 +/- 0.8	10.3 +/- 0.3	10 +/- 1

a bright future analytically for trace elemental analysis of real samples, particularly those requiring high selectivity.

CHAPTER 7
FLUORESCENCE DIP SPECTROSCOPY IN THE ICP

Introduction

Stepwise excitation techniques that use two or more lasers to sequentially excite atoms, ions or molecules to high levels are characterized by both high spatial and high spectral resolution and are therefore popular for combustion diagnostic and plasma diagnostic applications. Fluorescence dip spectroscopy is a technique that uses stepwise excitation to study the excited state of an atom, ion or small molecule by monitoring the decrease or dip in the laser induced fluorescence emission from an excited state when a second laser is used to probe excited state transitions from the fluorescent level [52]. When the second laser is tuned to an excited state transition that originates from the fluorescent level, the population of that level is depleted as the analyte species are promoted to a higher level which reduces the emission from the fluorescent level and is the basis of the fluorescence dip. The magnitude of the dip is dependent on several factors many of which are related specifically to the analyte species.

ICP-LIF has been used to profile atom and ion populations in the ICP and for excited state lifetime determinations [78,79]. The fluorescence dip is not only useful for gross physical measurements in flames and plasmas, such as number density and temperature determinations, but can be used to obtain fundamental physical information about the excited states of atomic and molecular species. The need for fundamental data in atomic fluorescence spectrometry, particularly LIF, was addressed recently [80]. As the author pointed out, the amount of information available for most elements is often limited or incomplete, and what information is available is usually obtained under experimental conditions that are not necessarily relevant to analytical applications. As the popularity of two color laser induced fluorescence (LIF) and laser enhanced ionization (LEI) experiments increases, the need for such information to be accurate and complete becomes greater as well.

It has been proposed that the fluorescence dip can be used to study excited state transitions in much the same way as saturated fluorescence measurements can be used to study ground state transitions [52]. The fluorescence dip has been used simultaneously with LEI to accurately determine the energies of Rydberg levels of nitric oxide molecules in a supersonic jet [81-83]. It was found that absorption cross sections could also be determined for excited state transitions reaching those levels. LEI and LIF dip measurements have been used to study Sr atoms and Li atoms in an air acetylene flame [84,85]. The results of these studies have been used to model the physical processes primarily responsible for signals in LEI and LIF with considerable success. It has been observed by several different authors that a fluorescence dip is often associated with an enhancement in the LEI signals, which has led to a better understanding of the ionization, fluorescence and collisional decay processes of excited atoms and molecules [86].

A novel application of the fluorescence dip has been reported where the dip is used to profile the concentration of atomic hydrogen in flames. The technique, known as photoionization controlled-loss spectroscopy (PICLS), makes photoionization the primary loss mechanism in the excited state [87]. Changes in the fluorescence intensity from the excited state allow an accurate evaluation of the concentration of hydrogen atoms independent of quenching rates. The fluorescence dip has also been used to determine the quantum efficiencies of several excited state transitions of sodium atom in the inductively coupled plasma (ICP) as well as to estimate the relative contributions of other non radiative de-excitation processes in the excited state of sodium [88].

Laser induced fluorescence dip spectroscopy has been used to study the excited states of silver, copper, palladium, iridium and lead atoms in the ICP. The results of these studies will be presented to demonstrate how this spectroscopy is capable of providing important physical information that can be used to characterize the excited states of atoms.

Results

Silver, copper, palladium, iridium and lead have each been studied by laser induced fluorescence dip spectroscopy in the ICP. Several important physical parameters have been evaluated for each element by using this technique and a summary of the results is shown in Table 6. The results provide valuable information about the excited state of each of these elements and give some idea of how these

Table 6

Summation of results for fluorescence dip studies of Ag, Cu, Pd, Ir and Pb

ELEMENT	Δ'_{cal}	Δ'_{obs}	ΔE_{IP} (eV)	Y_{32}^{a}	Δ'^{a}	$\rho^{s}_{\nu}(\upsilon)$ J/M^3Hz^{-1}	Y_{32}^{b}
Ag	0.56	0.52	1.53	0.0020	0.50	1.9×10^{-11}	0.0024
Cu	0.50	0.50	1.53	0.14	0.35	4.0×10^{-13}	0.15
Pd	0.39	0.45	1.51	0.0054	0.41	1.9×10^{-11}	0.0029
Ir	0.69	0.72	2.49	0.0025	0.74	1.5×10^{-11}	0.0021
Pb	0.38	0.41	0.97	0.00030	0.40	1.1×10^{-10}	0.00045

a. Y_{32} and Δ' values determined from slope and Y-intercept, respectively, of quantum efficiency plot.

b. Y_{32} determined from steady state saturation dip parameter, $\rho^{s}_{\nu}(\nu)$.

elements behave in a plasma environment. It is also interesting to compare the results predicted by the model based on the rate equations approach to the experimentally observed results and speculate on the reasons why they may differ.

For silver, copper and iridium, the maximum relative dips predicted by the model agree well with the experimental values. For most of the elements studied, there are several energy levels in the excited state that are close in energy and it is important to consider the effects of collisions. To account for possible coupling or mixing of levels, levels that are relatively close are often assumed to be well mixed and are viewed as a single conglomerate level which has a statistical weight (effective g) that is the sum of the statistical weights of all the individual levels which are mixed. In the ICP, collisions are usually considered to be less important and less effective than in flames mostly for the reason that the ICP operates on argon which is monatomic and therefore has a small collision cross section. Collisional coupling in the ICP has been studied previously [67] and found to be relatively insignificant for levels separated by much more than 1 eV, whereas in flames, efficient coupling has been observed by thermally assisted fluorescence for levels separated by over 2 eV.

Shown in Figures 16-20 are partial energy level diagrams for the five elements studied and the levels that are most likely to be collisionally coupled. For silver and copper, the number of levels that have a high probability for mixing is limited and the effective g for the excited states are easy to estimate. For iridium, the situation is complicated by a large number of levels, but by assuming that level mixing is not

Figure 16. Partial energy level diagram of Ag dip.

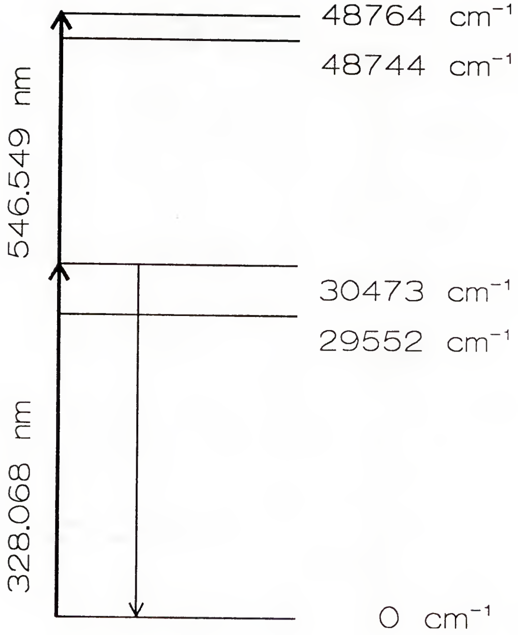
48764 cm⁻¹
48744 cm⁻¹
30473 cm⁻¹
29552 cm⁻¹
0 cm⁻¹
546.549 nm
328.068 nm

Figure 17. Partial energy level diagram of Cu dip.

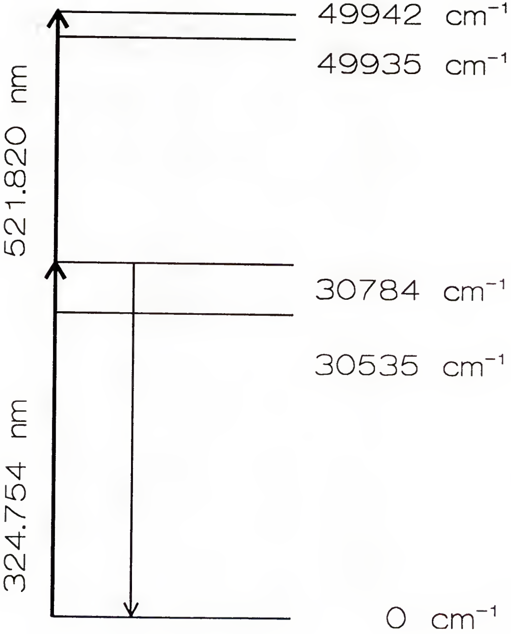
49942 cm^{-1}
49935 cm^{-1}
521.820 nm
30784 cm^{-1}
30535 cm^{-1}
324.754 nm
0 cm^{-1}

Figure 18. Partial energy level diagram of Pd dip.

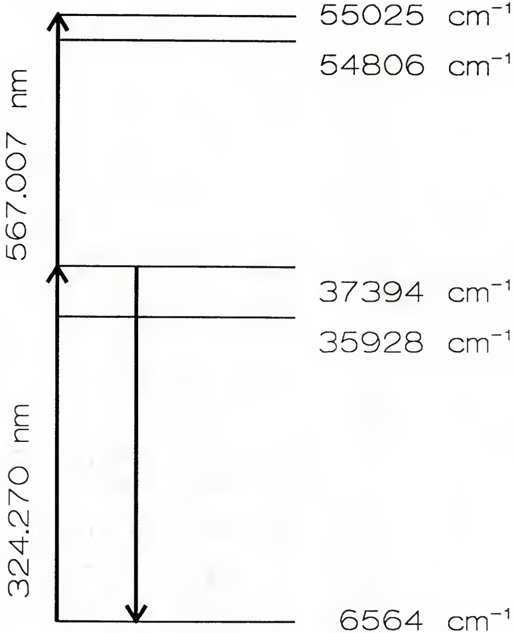
55025 cm⁻¹
54806 cm⁻¹
567.007 nm
37394 cm⁻¹
35928 cm⁻¹
324.270 nm
6564 cm⁻¹

Figure 19. Partial energy level diagram of Ir dip.

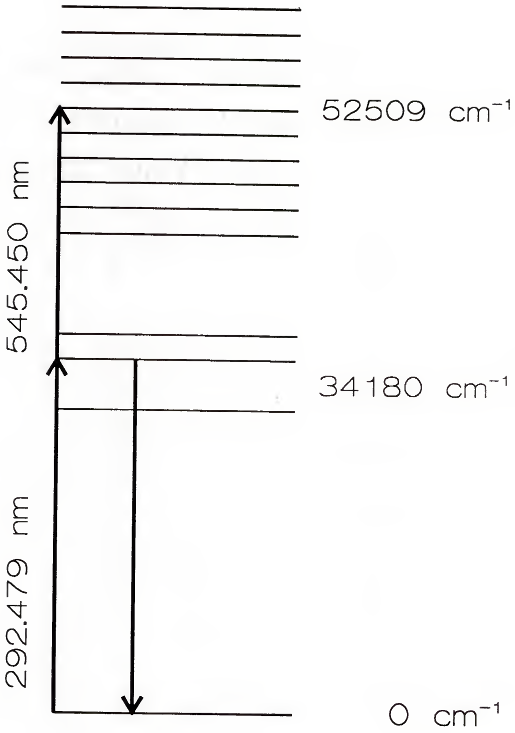
52509 cm⁻¹
545.450 nm
34180 cm⁻¹
292.479 nm
0 cm⁻¹

Figure 20. Partial energy level diagram of Pb dip.

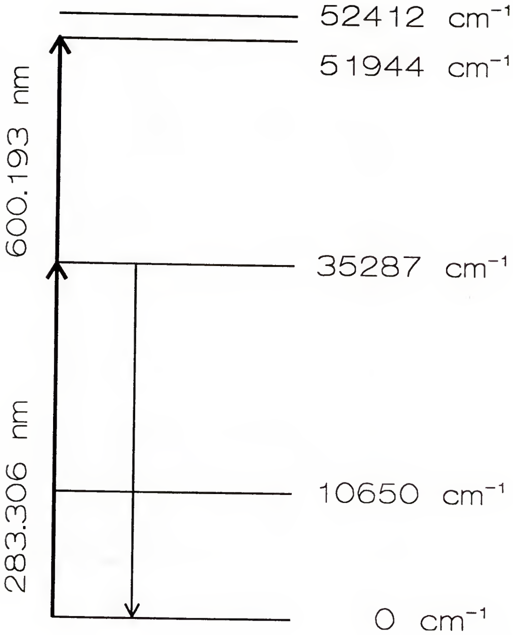
52412 cm⁻¹
51944 cm⁻¹
35287 cm⁻¹
10650 cm⁻¹
0 cm⁻¹
600.193 nm
283.306 nm

significant for levels beyond 0.2 eV away from the levels populated by the lasers, effective g values were calculated for iridium which resulted in an accurate prediction of the observed maximum relative dip. For palladium and lead, the number of levels available for mixing is also numerous, but the situation is further complicated by strong transitions to metastable levels and/or ionization processes that act as a trap to the atom population and prevent the level populations from reaching a steady state condition. Because of the time dependent nature of the fluorescence dip for these two elements, there is less agreement with the steady state predictions than with the other elements. Perhaps a more useful study for these elements would be to perform either a time resolved or a time integrated fluorescence dip measurement, neither of which was used in this study.

An important loss mechanism that must be considered for any two step fluorescence method is ionization from the highest level populated, which can occur either by collisions or by direct photoionization. While collisional ionization in flames is highly efficient for atoms that are promoted to within approximately 1 eV of the ionization limit, it is unclear how favorable this process is in the ICP. It is assumed that this is not a high probability process for the elements investigated because of the relatively large energy separation (1.5 eV) between the highest excited level populated by the laser and the ionization limit (column 3 of Table 6), with the exception of lead which is promoted to within 0.9 eV of the ionization limit. Collisional ionization is also unlikely because of the small collision cross section of argon.

Direct photoionization is a consideration for all of the elements studied, since the photon energy of the second step is greater than half of the energy required to reach the ionization limit and a two photon absorption of the second step could promote the one step excited atom into the ionization continuum. The only exception to both the collisional and photoionization losses is iridium, which is separated by such a large energy difference from the ionization limit that it would require either a three photon absorption of the second step or a highly energetic collision to be ionized, both of which are very unlikely.

The steady state saturation dip parameter, ρ_ν^s, is a parameter that was evaluated for each of the elements by plotting the log of the relative fluorescence dip observed against the log of the spectral energy density of ν_{23}. This plot takes the form of a saturation curve which is characterized by two linear regions, one line at low spectral energy densities and a linear plateau region at higher spectral energy densities. If these two lines are extrapolated, their point of intersection should occur at a spectral energy density that corresponds to a relative dip equal to one half the maximum relative dip. This spectral energy density is defined as the steady state saturation dip parameter and is analogous to the saturation spectral energy density determined from saturation curves for one step excited fluorescence measurements. The quantum efficiency of fluorescence for the second step excitation can be evaluated from the steady state saturation dip parameter using equation 63. Fluorescence dip saturation curves were plotted for each of the elements (figures 21-25). The steady state saturation dip parameters and the quantum efficiencies have

Figure 21. Ag dip saturation curve.

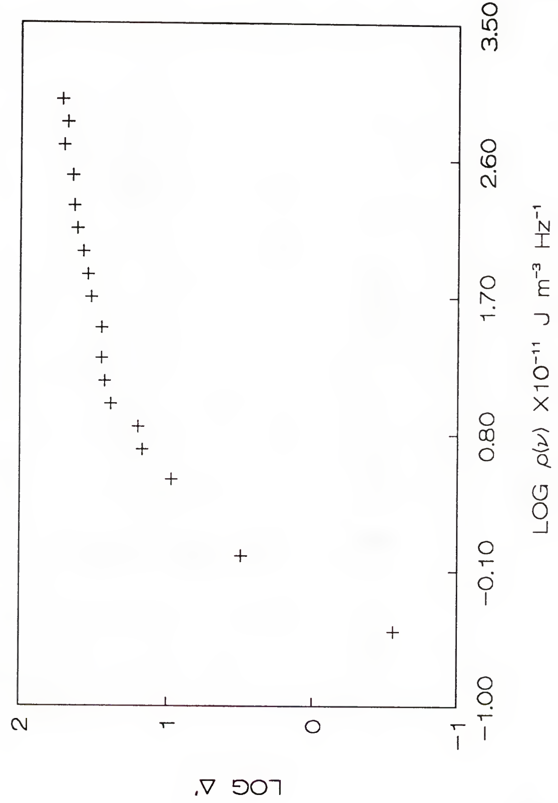
LOG Δ'
2
1
0
−1
−1.00
−0.10
0.80
1.70
2.60
3.50
LOG ρ(ν) X10⁻¹¹ J m⁻³ Hz⁻¹

Figure 22. Cu dip saturation curve.

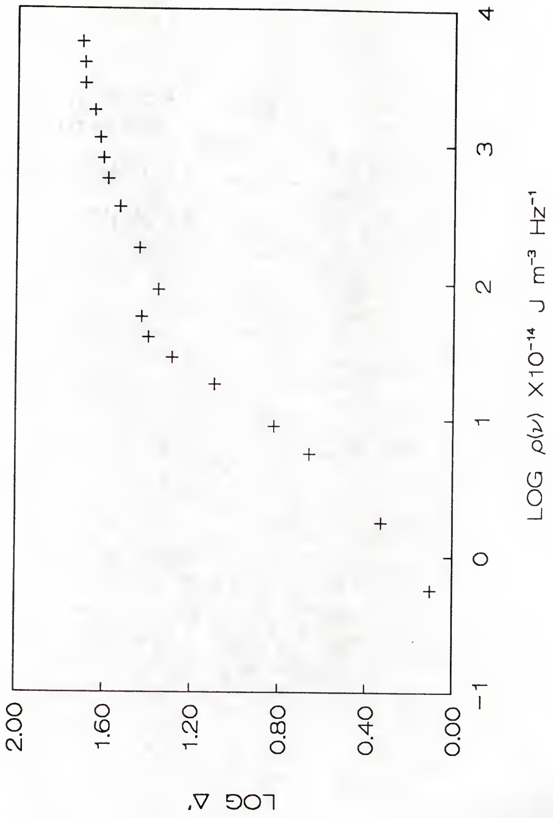
LOG Δ'
2.00
1.60
1.20
0.80
0.40
0.00
−1
0
1
2
3
4
LOG ρ(ν) X10^-14 J m^-3 Hz^-1

Figure 23. Pd dip saturation curve.

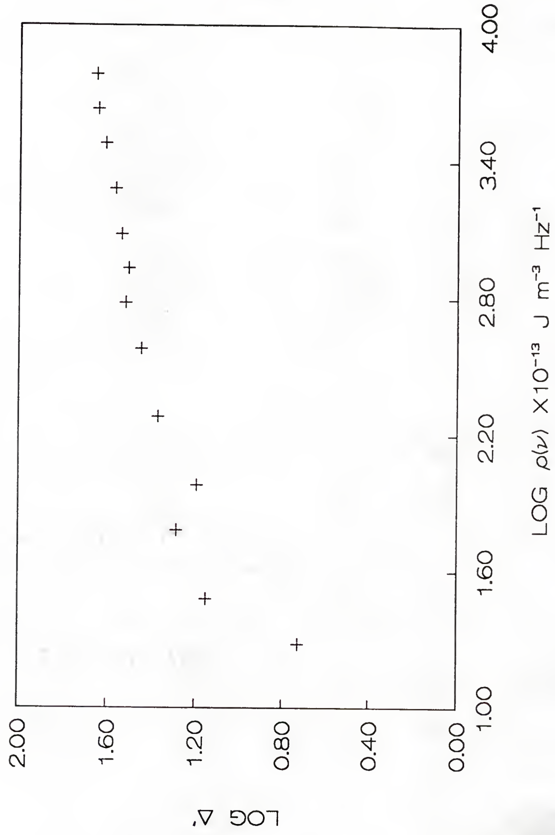
LOG Δ'
2.00
1.60
1.20
0.80
0.40
0.00
1.00
1.60
2.20
2.80
3.40
4.00
LOG ρ(ν) X10⁻¹³ J m⁻³ Hz⁻¹

Figure 24. Ir dip saturation curve.

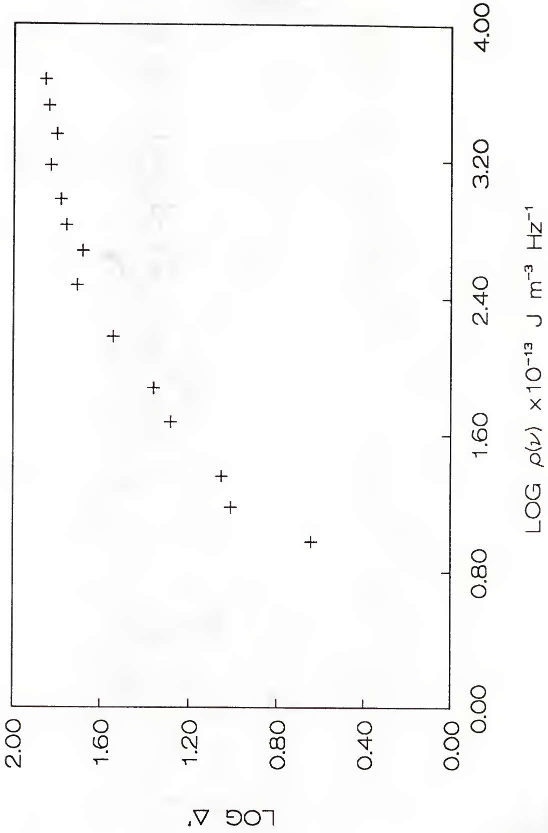
LOG Δ'
2.00
1.60
1.20
0.80
0.40
0.00
0.00
0.80
1.60
2.40
3.20
4.00
LOG $\rho(\nu)$ ×10^{-13} J m^{-3} Hz^{-1}

Figure 25. Pb dip saturation curve.

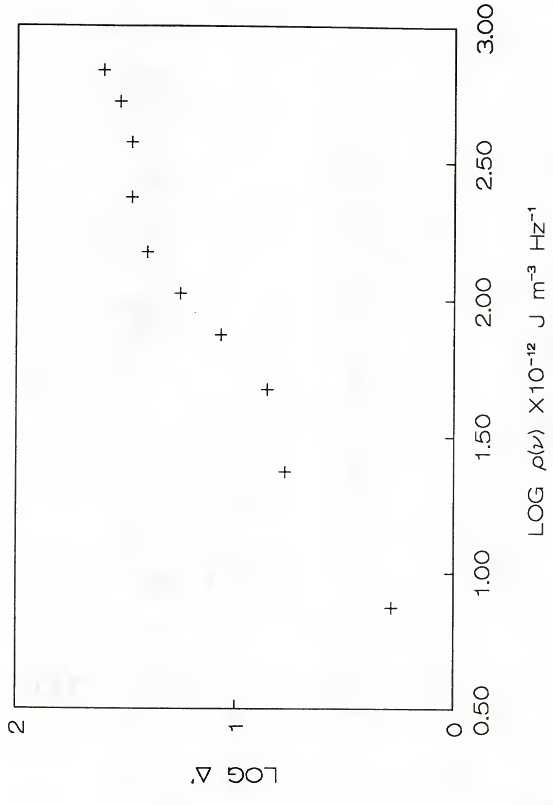
LOG Δ'
0
1
2
0.50
1.00
1.50
2.00
2.50
3.00
LOG ρ(ν) X10⁻¹² J m⁻³ Hz⁻¹

been determined from the saturation curves for all five elements and are listed in column 7 and column 8 respectively, of Table 6.

From equation 64, it is seen that a plot of $(\Delta')^{-1}$ against the inverse of the spectral energy density of ν_{23} should produce a line, the slope of which can be used to determine the quantum efficiency while the intercept should be equal to the inverse of the maximum relative fluorescence dip. These so called quantum efficiency plots were generated for each of the five elements [Figures 26-30]. The quantum efficiencies and maximum relative dips determined from the plots are listed in column 5 and column 6, respectively, of Table 6. The plots were all characterized by good linearity with the average correlation coefficient being about 0.98. The maximum relative dips determined from the intercepts of the linear plots are in good agreement with those obtained directly from the dip measurements and the quantum efficiencies determined from the plots are also in very good agreement with those determined from the steady state saturation dip parameters.

There are interesting conclusions that can be drawn from these results. First, the rate equations model of the fluorescence dip is able to predict the experimentally observed results very well. The high degree of correlation of the quantum efficiency plots as well as the close similarity between the two types of quantum efficiency determinations support the steady state model. From element to element, it is striking how much the quantum efficiencies differ. The values range from 0.00026 for lead to 0.15 for copper which indicates significant differences in the roles of collisions, metastable levels and ionization losses for individual elements. The

Figure 26. Ag quantum efficiency plot.

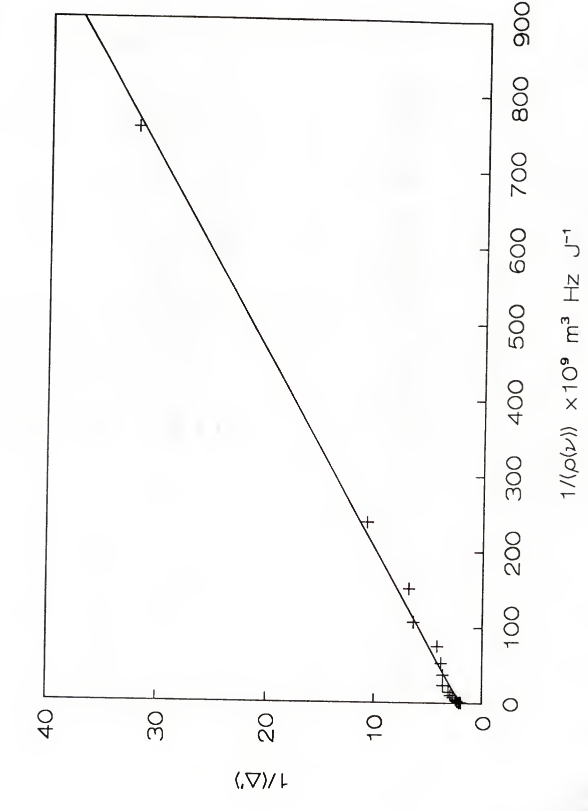
1/⟨Δ'⟩
0
10
20
30
40
0
100
200
300
400
500
600
700
800
900
1/⟨ρ(ν)⟩ ×10⁹ m³ Hz J⁻¹

Figure 27. Pb quantum efficiency plot.

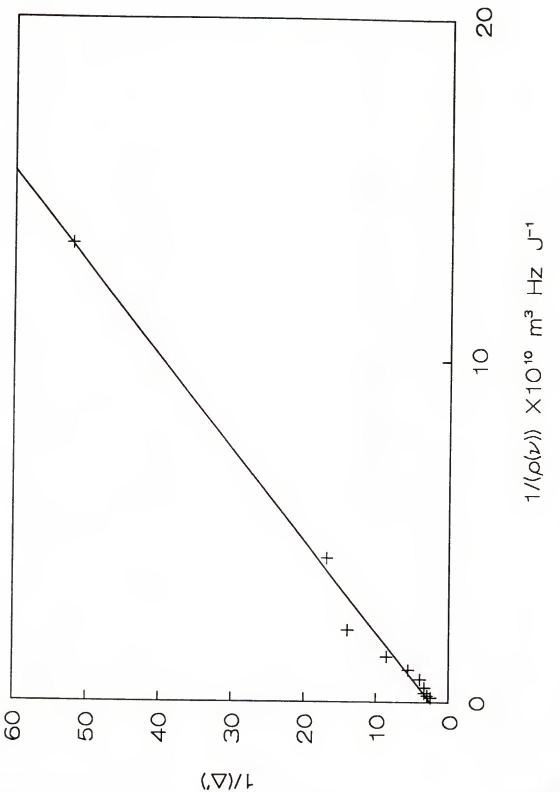
1/(Δν')
0
10
20
30
40
50
60
0
10
20
1/(ρ(ν)) ×10¹⁰ m³ Hz J⁻¹

Figure 28. Cu quantum efficiency plot.

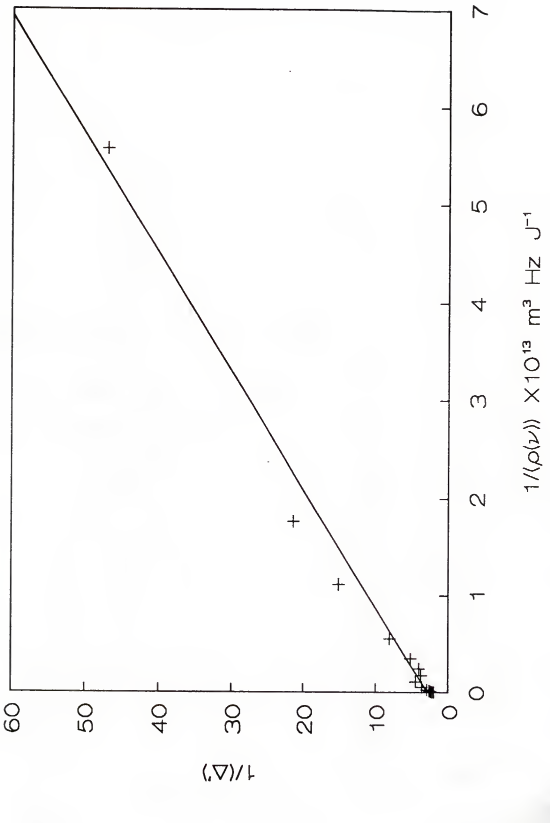
1/(Δ')
0
10
20
30
40
50
60
0
1
2
3
4
5
6
7
1/⟨ρ(ν)⟩ ×10^{13} m^3 Hz J^{-1}

Figure 29. Pd quantum efficiency plot.

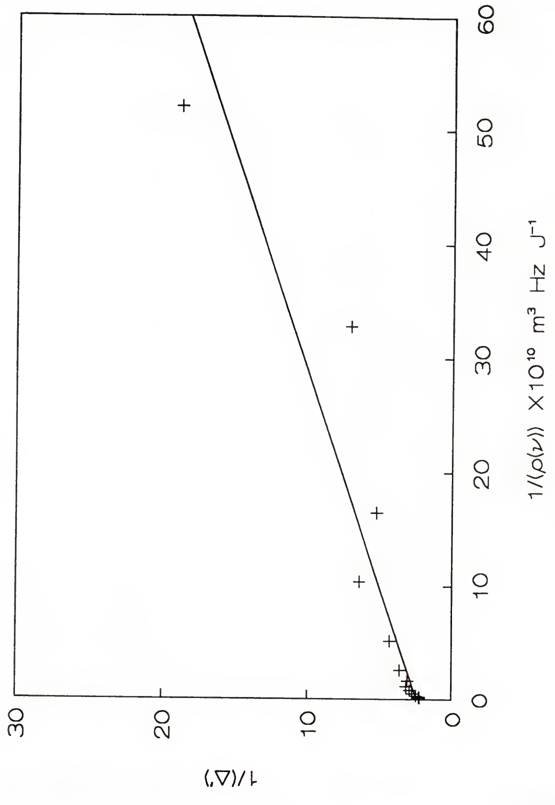

1/(Δ')
0
10
20
30
0
10
20
30
40
50
60
1/(ρ(ν)) ×10¹⁰ m³ Hz J⁻¹

Figure 30. Ir quantum efficiency plot.

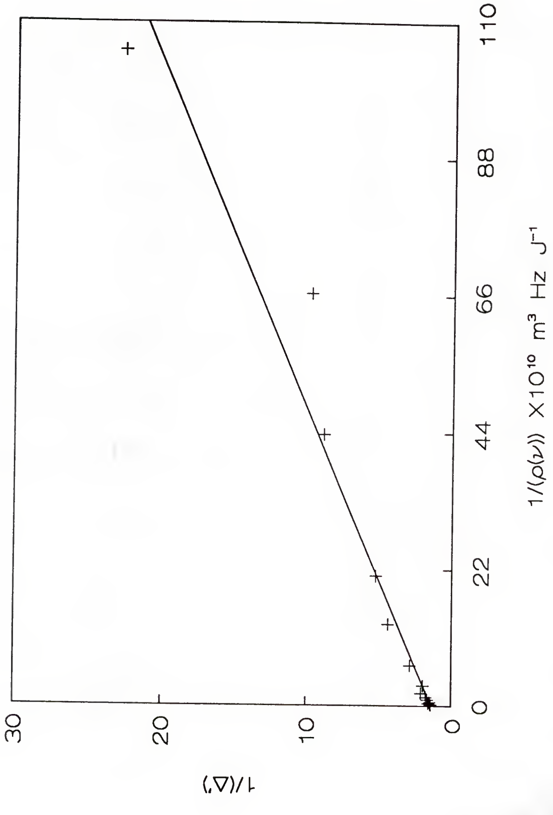
1/(Δ')
0
10
20
30
0
22
44
66
88
110
1/(ρ(ν)) ×10¹⁰ m³ Hz J⁻¹

relatively high quantum efficiency of copper suggests that there are very few net losses in the two step excitation/relaxation processes. It appears that the atom population density is efficiently recycled and the level population densities reach a steady state during the laser pulse. Since copper atom is a relatively simple atom in terms of electronic structure, it is not surprising that it has the highest quantum efficiency.

By comparison, the other four elements are more complex. They have many more levels in the excited state and are subject to several other loss mechanisms. Collisional redistribution of the atom population densities among many levels in the excited state lowers the quantum efficiency of fluorescence significantly. Losses to a metastable level also lowers the quantum efficiency. Ionization processes obviously lower the quantum efficiency since the ionization occurs in lieu of fluorescence. With these processes in mind, it is easy to understand why the quantum efficiencies are as low as they are for certain elements. For silver and palladium, the quantum efficiencies are lowered because of collisional redistributions. Ionization is possible, but is probably unlikely when the energy difference is over 1.5 eV for both elements. The case for iridium is similar for the same reasons. Iridium has a very large number of levels in the upper excited state, all of which have large statistical weights and will mix efficiently with the laser populated level and coupling by these levels lowers the quantum efficiency. As mentioned before, ionization losses are very minimal for iridium which must overcome a 2.5 eV energy separation. There is expected to be a significant amount of collisional coupling in the excited state for lead, which will suppress the quantum efficiency. Unlike the other elements though, lead is within 1 eV of the ionization limit and is expected to have a significant degree of losses due to ionization. It also has very strong relaxations to metastable levels which lower the quantum efficiency.

The losses to ionization and metastable levels are primarily responsible for the differences in the experimentally observed dips and those predicted by the steady state dip model. The model is based on an atom with three energy levels and does not account for these types of processes. Despite the limitations of the model, the assumption of steady state population densities is not a poor one, since the dip in most cases will not show effects of these processes in the early stages of the laser pulse. By limiting the experimental observation time to the first few nanoseconds of the laser pulse, it is possible to assume "quasi-steady state" conditions and obtain dip information that is relatively independent of these processes.

Time Dependent Fluorescence Dip Spectroscopy

The fluorescence dip can also be used to evaluate the Einstein coefficients for absorption and spontaneous emission of the second excitation step in the two step scheme. Using equation 65 and the correct experimental parameters, it is possible to solve for B_{23}. It is a straightforward calculation to determine both A_{32}, the coefficient for spontaneous emission, and f_{23}, the absorption oscillator strength, from B_{23} using equations 67 and 66 respectively. If the number densities of the atom are transient during the laser pulse, then an accurate evaluation of B_{23} requires an integrated fluorescence dip measurement. However, if the atom can be forced into a steady state dip, then a "peak" fluorescence dip measurement will suffice, since the peak dip will accurately reflect the integrated dip throughout the laser pulse.

Based on the dip results obtained, copper alone appears to be described reasonably by a three level atom. By numerically evaluating equation 65, values for B_{23}, A_{32} and f_{23} of the second transition of each of the elements studied were determined. Only the copper results were in good agreement with values found in the literature. These values are shown in Table 7. Literature values for A_{32} and f_{23} are also shown for comparison purposes. Based on the results, the assumption of steady state population densities throughout the laser pulse appears to be valid only for copper atom, which is reasonable considering the simplistic nature of the atom.

It is worth noting however, that while there are differences between the dip determinations and the literature results, the values for the Einstein coefficients and oscillator strengths reported in the literature are not necessarily correct, since measurements of these parameters are from arc emission spectra, which is often inaccurate for excited state transition determinations. The ability to accurately determine fundamental information is a strong attribute of the fluorescence dip method, which should be expected to find many more such applications in the future.

Table 7

Evaluation of Einstein coefficients for an excited state transition of Cu using time integrated fluorescence dip measurements

λ=521.820 nm

	$B_{23(obs)}$ $J^{-1}m^3Hzs^{-1}$	$A_{32(obs)}$ s^{-1}	$A_{32(lit)}$[a] s^{-1}	gf_{obs}	gf_{lit}[a]
Cu	2.3×10^{20}	2.7×10^{7}	9.7×10^{7}	0.7	2.4

a. C.H. Corliss and W.R. Bozman, NBS Monograph 53, 1962 [77].

CHAPTER 8
CONCLUSIONS

ICP-LIF has been demonstrated as a powerful spectrochemical method of analysis. The method is both highly selective and highly sensitive which is uncommon for most elemental methods. The studies performed for this work have shown a few of the many possible applications of ICP-LIF for analysis of complex samples and for diagnostics.

The study of selected rare earth elements is particularly interesting. The potential for spectral interferences in LIF has not been given much attention in the past, primarily because of the high selectivity of the method. However, as LIF applications to elemental analysis increase, it is likely that spectral interferences due to saturation broadening will occur. As the experimental results indicate, consideration needs to be given to narrow bandwidth laser systems, especially those that have high spectral energy densities.

The major conclusion that can be drawn from the double resonance fluorescence experiments is that collisions play a large role in the dynamics of atomic and ionic species in the ICP. Collisional coupling and mixing of excited states will often lower the sensitivity of ICP-LIF. For elements having simple electronic structures that can be approximated by a three level atom, collisions in the ICP apparently are not a major concern. For elements having several closely spaced levels in the excited state, collisions can be very important. When developing a double resonance excitation scheme for maximum sensitivity, attention should be given to possible collisional coupling.

Collisional redistributions can sometimes enhance the selectivity of ICP-LIF. Double resonance excitation often produces unique fluorescence excitation and fluorescence emission spectra which may be used for spectral identification of the elements. The high selectivity of the excitation process virtually guarantees that the observed fluorescence emission is due to the analyte alone. Such high selectivities are very useful for measurements of real samples, as the analysis of a standard reference material demonstrated.

LIF is already a popular tool for combustion diagnostic studies in flames but has not been explored fully in the ICP. Double resonance fluorescence spectrometry, fluorescence dip spectroscopy and pump-probe spectroscopy are all methods that can find numerous applications in the ICP. Fluorescence dip spectroscopy is an excellent example of a relatively simple but powerful method that can provide a large amount of important physical information. While the studies performed for this work focussed on peak fluorescence dip measurements, time integrated dip measurements are also possible which allow evaluation of excited state lifetimes and nonradiative deactivation rates.

Future areas of research for ICP-LIF include further applications to real samples for both single resonance and double resonance excitation techniques. For the rare earth elements, the problem of spectral interferences caused by saturation broadening of the excitation profiles should be studied systematically. The relative importance of factors such as narrow and broad bandwidth laser excitation, source spectral energy density changes and the interferant concentration dependence should all be addressed. Attention should also be given to the possibility of double resonance fluorescence for rare earth elements for improved selectivity.

Future diagnostic studies using ICP-LIF include application of fluorescence dip spectroscopy to ionic as well as other atomic species. Time integrated and time resolved fluorescence dip measurements are promising methods for the accurate determination of ionization and nonradiative deactivation rates. Variations of the fluorescence dip are also possible. The use of a multiphoton absorption as the primary absorption followed by absorption of ionizing or nonionizing radiation could conceivably allow the measurement of a dip in stimulated emission rather than fluorescence emission. Stimulated emission techniques are already used for the analysis of nonmetals in flames and their application to the ICP is reasonable.

REFERENCE LIST

1. J.C. Van Loon, "Selected Methods of Trace Analysis," Wiley, New York, 1985.
2. N. Omenetto, Spectrochim. Acta 44B, 131, 1989.
3. R.K. Winge, V.J. Peterson and V.A Fassel, Appl. Spectrosc. 33, 206, 1979.
4. J. Luck and U. Siewers, Fresenius Z. Anal. Chem. 331, 129, 1988.
5. J. Takahashi and R. Hara, Analytical Sciences 4, 331, 1988.
6. A.C. Eckbreth, P.A. Bonczyk and J.F. Verdieck, "Laser Raman and Fluorescence Techniques for Practical Combustion Diagnostics," Appl. Spectrosc. Reviews 13, 15, 1978.
7. R.M. Measures, J. Appl. Phys. 39, 5232, 1968.
8. M.B. Denton and H.V. Malmstadt, Appl. Phys. Lett. 18, 485, 1971.
9. L.M. Fraser and J.D. Winefordner, Anal. Chem. 43, 1693, 1971.
10. J. Kuhl, G. Marowsky and R. Torge, Anal. Chem. 44, 375, 1972.
11. E.H. Piepmeier, Spectrochim. Acta 27B, 431, 1972.
12. L.M. Fraser and J.D. Winefordner, Anal. Chem. 44, 1444, 1972.
13. M. Heaven, T.A. Miller, R.R. Freeman, J.C. White and J. Bokor, Chem. Phys. Lett. 86, 458, 1982.
14. M. Alden, H. Edner, P. Grafstrom and S. Svanberg, Opt. Comm. 42, 244, 1982.
15. R.P. Lucht, J.T. Salmon, G.B. King, D.W. Sweeney and N.M. Laurendeau, Opt. Lett. 8, 365, 1983.

16. M. Alden, A.L. Schalow, S. Svanberg, W. Wendt and P.L. Zhang, Opt. Lett. 9, 211, 1984.

17. A.W. Miziolek and M.A. DeWilde, Opt. Lett. 9, 390, 1984.

18. G.C. Herring, M.J. Dyer, L.E. Jusinski and W.K. Bischel, Opt. Lett. 13, 360, 1988.

19. J.E.M. Goldsmith, R.J.M. Anderson and L.R. Williams, Opt. Lett. 15, 78, 1990.

20. J.E.M. Goldsmith and N.M. Laurendeau, Opt. Lett. 15, 576, 1990.

21. S. Agrup, U. Westblom and M. Alden, Chem. Phys. Lett. 170, 406, 1990.

22. N. Omenetto, N.N. Hatch, L.M. Fraser and J.D. Winefordner, Spectrochim. Acta 28B, 65, 1973.

23. N. Omenetto, P. Benetti, L.P. Hart, J.D. Winefordner and C.Th.J. Alkemade, Spectrochim. Acta 28B, 289, 1973.

24. G.D. Boutilier, M.B. Blackburn, J.M. Mermet, S.J. Weeks, H. Haraguchi, J.D. Winefordner and N. Omenetto, Appl. Opt. 17, 2291, 1978.

25. S.J. Weeks, H. Haraguchi and J.D. Winefordner, Anal. Chem. 50, 360, 1978.

26. S. Neumann and M. Kriese, Spectrochim. Acta 29B, 127, 1974.

27. M.A. Bolshov, A.V. Zybin and I.I. Smirenkina, Spectrochim. Acta 36B, 1143, 1981.

28. F.R. Preli, J.P. Dougherty and R.G. Michel, Anal. Chem. 59, 1784, 1987.

29. M. Leong, J. Vera, B.W. Smith, N. Omenetto and J.D. Winefordner, Anal. Chem. 60, 1605, 1988.

30. M.A. Bolshov, A.V. Zybin, V.G. Koloshnikov and I.I. Smerinkina, Spectrochim. Acta 43B, 519, 1988.

31. N. Omenetto, B.W. Smith and J.D. Winefordner, Spectrochim. Acta 43B, 1111, 1988.

32. A. Montaser and V.A. Fassel, Anal. Chem. 48, 1490, 1976.

33. B.D. Pollard, M.B. Blackburn, S. Nikdel, A. Massoumi and J.D. Winefordner, Appl. Spectrosc. 33, 5, 1979.

34. M.S. Epstein, S. Nikdel, J.D. Bradshaw, M.A. Kosinski, J.N. Bower and J.D. Winefordner, Anal. Chim. Acta 113, 221, 1980.

35. M.A. Kosinski, H. Uchida and J.D. Winefordner, Talanta 30, 339, 1983.

36. D.R. Demers and C.D. Allemand, Anal. Chem. 53, 1915, 1981.

37. D.R. Demers, Spectrochim. Acta 40B, 93, 1985.

38. D.R. Demers, American Laboratory (August), 30, 1987.

39. C.Th.J. Alkemade, Tj Hollander, W. Snelleman and P.J.Th. Zeegers, "Metal Vapours in Flames," Pergamon Press, Oxford, 1982.

40. N. Omenetto and J.D. Winefordner, Prog. Anal. At. Spectrosc. 2, 1, 1979.

41. N. Omenetto and J.D. Winefordner, in "Analytical Laser Spectroscopy," Ed. N. Omenetto, Chap. 4, Wiley, New York, 1979.

42. J.W. Daily, Appl. Opt. 16, 2322, 1977.

43. J.W. Daily, Appl. Opt. 17, 225, 1978.

44. P.W. Atkins, "Physical Chemistry," W.H. Freeman and Co., San Francisco, 1982.

45. N. Omenetto, B.W. Smith, L.P. Hart, P. Cavalli and G. Rossi, Spectrochim. Acta 40B, 1411, 1985.

46. P.W.J.M. Boumans, J.A. Tielrooy and F.J.M.J. Maessen, Spectrochim. Acta 43B, 173, 1988.

47. C.A. Van Dijk, Ph.D. Thesis, University of Utrecht, 1978.

48. N. Omenetto, J. Bower, J. Bradshaw, C.A. Van Dijk and J.D. Winefordner, J. Quant. Spectrosc. Radiat. Transfer 24, 147, 1980.

49. N. Omenetto, J. Bower, J. Bradshaw, S. Nikdel and J.D. Winefordner, "Laser Probes for Combustion Chemistry," Ed. D.R. Crosley, ACS Symposium Series 134, Washington, DC, 1980.

50. C.Th.J. Alkemade and T. Wijchers, Anal. Chem. 49, 2111, 1977.

51. J.W. Hosch and E.H. Piepmeier, Appl. Spectrosc. 32, 444, 1978.

52. N. Omenetto, G.C. Turk, M. Rutledge and J.D. Winefordner, Spectrochim. Acta 42B, 807, 1987.

53. A.P. Thorne, "Spectrophysics," Chapman and Hall, London, 1988.

54. H. Qing-Lie, T.C. Hughes, M. Haukka and P. Hannaker, Talanta 32, 495, 1985.

55. J. Broekaert and P. Hormann, Anal. Chim. Acta 124, 421, 1981.

56. J.G. Crock and F.E. Lichte, Anal. Chem. 54, 1329, 1982.

57. A. Bolton, J. Hwang and A. Vander Voet, Spectrochim. Acta 38B, 165, 1983.

58. S.J. Buchanan and L.S. Dale, Spectrochim. Acta 41B, 237, 1986.

59. D.W. Zachmann, Anal. Chem. 60, 420, 1988.

60. P.W.J.M. Boumans, J.J.A.M. Vrakking and A.H.M. Heijms, Spectrochim. Acta 43B, 1365, 1988.

61. P.W.J.M. Boumans, H. ZhiZhuang, J.J.A.M. Vrakking, J.A. Tielrooy and F.J.M.J. Maessen, Spectrochim. Acta 44B, 31, 1989.

62. N. Omenetto, N.N. Hatch, L.M. Fraser and J.D. Winefordner, Anal. Chem. 45, 195, 1973.

63. M.E. Tremblay, B.W. Smith and J.D. Winefordner, Anal. Chim. Acta 199, 111, 1987.

64. M.E. Tremblay, J.B. Simeonsson, B.W. Smith and J.D. Winefordner, Appl. Spectrosc. 42, 281, 1988.

65. B.W. Smith, M.R. Glick, K.N. Spears and J.D. Winefordner, Appl. Spectrosc. 43, 376, 1989.

66. Thermo Jarrell Ash commercial literature, 1987.

67. H. Uchida, M.A. Kosinski, N. Omenetto and J.D. Winefordner, Spectrochim. Acta 39B, 63, 1984.

68. P.W.J.M. Boumans, Fresenius Z. Anal. Chem. 324, 397, 1986.

69. P.W.J.M. Boumans and J.J.A.M. Vrakking, Spectrochim. Acta 41B, 1235, 1986.

70. N. Omenetto, H.G.C. Human, P. Cavalli and G. Rossi, Spectrochim. Acta 39B, 115, 1984.

71. H.G.C. Human, N. Omenetto, P. Cavalli and G. Rossi, Spectochim. Acta 39B, 1345, 1984.

72. X. Huang, J. Lanauze and J.D. Winefordner, Appl. Spectrosc. 39, 1042, 1985.

73. N. Omenetto, B.W. Smith and L.P. Hart, Fresenius Z. Anal. Chem. 324, 683, 1986.

74. N. Omenetto and H.G.C. Human, Spectrochim. Acta 39B, 1333, 1984.

75. M.A. Kosinski, H. Uchida and J.D. Winefordner, Talanta 30, 339, 1983.

76. H. Uchida, M.A. Kosinski and J.D. Winefordner, Spectrochim. Acta 38B, 5, 1983.

77. C.H. Corliss and W.R. Bozman, NBS Monograph 53, 1962.

78. N. Omenetto, S. Nikdel, R.D. Reeves, J. Bradshaw, J. Bower and J.D. Winefordner, Spectrochim. Acta 35B, 507, 1980.

79. H. Uchida, M.A. Kosinski, N. Omenetto and J.D. Winefordner, Spectrochim. Acta 38B, 529, 1983.

80. N. Omenetto, Spectrochim. Acta 43B, 63, 1988.

81. T. Ebata, N. Mikami and M. Ito, J. Chem. Phys. 78, 1132, 1983.

82. Y. Anezaki, T. Ebata, N. Mikami and M. Ito, Chem. Phys. 89, 103, 1984.

83. Y. Anezaki, T. Ebata, N. Mikami and M. Ito, Chem. Phys. 97, 153, 1985.

84. B.W. Smith, L.P. Hart and N. Omenetto, Anal. Chem. 58, 2147, 1986.

85. G.C. Turk and N. Omenetto, Appl. Spectrosc. 40, 1085, 1986

86. O. Axner, M. Norberg and H. Rubinsztein-Dunlop, Spectrochim. Acta 44B, 693, 1989

87. J.T. Salmon and N.M. Laurendeau, Opt. Lett. 11, 419, 1986.

88. N. Omenetto, M. Leong, C. Stevenson, J. Vera, B.W. Smith and J.D. Winefordner, Spectrochim. Acta 43B, 1093, 1988.

BIOGRAPHICAL SKETCH

Josef B. Simeonsson was born April 27, 1964, in Chattanooga, Tennessee. He attended the University of North Carolina at Chapel Hill from 1982 to 1986 and graduated with a Bachelor of Science degree in chemistry. He entered graduate school in the Department of Chemistry at the University of Florida in 1986.

I certify that I have read this study and that in my opinion it conforms to acceptable standards of scholarly presentation and is fully adequate, in scope and quality, as a dissertation for the degree of Doctor of Philosophy.

James D. Winefordner

James D. Winefordner, Chairman
Graduate Research Professor of Chemistry

I certify that I have read this study and that in my opinion it conforms to acceptable standards of scholarly presentation and is fully adequate, in scope and quality, as a dissertation for the degree of Doctor of Philosophy.

Gerhard Schmid
Associate Professor of Chemistry

I certify that I have read this study and that in my opinion it conforms to acceptable standards of scholarly presentation and is fully adequate, in scope and quality, as a dissertation for the degree of Doctor of Philosophy.

Anna Brajter-Toth
Associate Professor of Chemistry

I certify that I have read this study and that in my opinion it conforms to acceptable standards of scholarly presentation and is fully adequate, in scope and quality, as a dissertation for the degree of Doctor of Philosophy.

Vaneica Young

Vaneica Young
Associate Professor of Chemistry

I certify that I have read this study and that in my opinion it conforms to acceptable standards of scholarly presentation and is fully adequate, in scope and quality, as a dissertation for the degree of Doctor of Philosophy.

Ralph Dawson Jr

Ralph Dawson
Assistant Professor of Pharmacodynamics

This dissertation was submitted to the Graduate Faculty of the Department of Chemistry in the College of Liberal Arts and Sciences and to the Graduate School and was accepted as partial fulfillment of the requirements for the degree of Doctor of Philosophy.

December, 1990

Dean, Graduate School